

DEVELOPMENT OF DYNAMIC INTESTINAL MODEL (DIM) FOR DIGESTION
KINETICS STUDIES

by

NATHANIEL DAVID WRIGHT

(Under the Direction of Fanbin Kong)

ABSTRACT

The human small intestine is a highly specialized organ for the digestion of food and absorption of nutrients. A dynamic Intestinal Model (DIM) was developed in this study with accurate simulation of segmentation contraction. The DIM was verified with pressure test as well as glucose absorption test to measure permeability. These results showed good correlation between results observed in DIM and from *in vivo* studies done by other researchers. Methylene blue was used to study intestinal digestion kinetics in DIM as related to factors including flow rate of digesta, temperature, viscosity, orientation and segmentation characteristics. Bread digestion was also carried out to study glucose release comparing DIM and commonly used method using shaking water bath to mix digesta. Results showed that a higher amount of glucose was generated in DIM and bile has a strong inhibitory effect in starch digestion.

INDEX WORDS: dynamic intestinal model; digestion kinetics; starch digestion

DEVELOPMENT OF DYNAMIC INTESTINAL MODEL (DIM) FOR DIGESTION
KINETICS STUDIES

by

NATHANIEL DAVID WRIGHT

B.S.A., University of Georgia, 2008

B.A., LaGrange College, 2005

A Thesis Submitted to the Graduate Faculty of The University of Georgia in Partial
Fulfillment of the Requirements for the Degree

MASTER OF SCIENCE

ATHENS, GEORGIA

2013

© 2013

Nathaniel David Wright

All Rights Reserved

DEVELOPMENT OF DYNAMIC INTESTINAL MODEL (DIM) FOR DIGESTION
KINETICS STUDIES

by

NATHANIEL DAVID WRIGHT

Major Professor: Fanbin Kong

Committee: William Kerr
Louise Wicker

Electronic Version Approved:

Maureen Grasso
Dean of the Graduate School
The University of Georgia
August 2013

DEDICATION

I dedicate this work to two special people in my life. First of all, I dedicate this to William Shelor Rodgers. He was an alumnus of UGA as well as a WWII Navy veteran and long-serving pharmacist. Most importantly, he was my grandfather. I know he would have been proud of my accomplishments here at his alma mater.

The second person I would like to dedicate this too is Dr. John Hurd. He not only was a great academic advisor to me back at LaGrange College but he was a good friend and kind soul that helped me through an emotional time during my senior year there. His passing came as a complete shock to me and I can think of no better way to remember him than to dedicate this work to him.

ACKNOWLEDGEMENTS

I want to thank most of all Dr. Fanbin Kong for his patient guidance in bringing this thesis to completion. I also acknowledge those I've worked with closely in sharing lab space including fellow students Floirendo, Eric, and Duc as well as tech VJ Sharma and post-doc Wei Zhao. It's been great working with these guys. Also thanks to the input and advice from both my committee members Dr. William Kerr and Dr. Louise Wicker.

TABLE OF CONTENTS

	Page
ACKNOWLEDGEMENTS	v
LIST OF TABLES.....	viii
LIST OF FIGURES	ix
CHAPTER	
1 REVIEW OF THE LITERATURE AND OBJECTIVES	1
Pre-Intestine Digestion Overview.....	1
Small Intestine Anatomy and Physiology.....	2
Dynamic Models for Simulating Intestinal Digestion.....	6
Digestion Kinetics	8
Enzyme Inhibition	8
Objectives of Study.....	9
References	11
2 DYNAMIC INTESTINAL MODEL DEVELOPMENT AND PRESSURE	
MEASUREMENT.....	13
Abstract	14
Introduction	14
Model Development.....	18
Protocol of DIM Operation	23
Materials and Methods	27
Results and Discussion	28

	Conclusions	32
	References	34
3	PERMEABILITY AND PROPAGATION PATTERNS OF METHYLENE BLUE IN DYNAMIC INTESTINAL MODEL (DIM)	36
	Abstract	37
	Introduction	37
	Materials and Methods	38
	Results and Discussion	43
	Conclusions	60
	References	61
4	COMPARISON OF SHAKING WATER BATH AND DYNAMIC INTESTINAL MODEL (DIM) IN SIMULATING STARCH DIGESTION AS AFFECTED BY GASTRIC DIGESTION AND BILE.....	63
	Abstract	64
	Introduction	64
	Materials and Methods	66
	Results and Discussion	71
	Conclusions	75
	References	76
5	OVERALL CONCLUSIONS	77

LIST OF TABLES

	Page
Table 1.1: Digestive system average lengths	5
Table 3.1: Permeability results from flow rate trial	45
Table 3.2: Permeability results from temperature trial.....	48
Table 3.3: Permeability results from viscosity trial.....	50
Table 3.4: Permeability results from segmentation placement trial.....	58

LIST OF FIGURES

	Page
Figure 1.1: Small intestine anatomy.....	4
Figure 1.2: Brush border enzymes of small intestine	5
Figure 1.2: TIM model of stomach and small intestine.....	7
Figure 1.3: SIM segmentation schematic.....	7
Figure 2.1: Organization of the wall of the small intestine into functional layers	15
Figure 2.2: Mixing action of segmentation contractions.....	16
Figure 2.3: Overall view of DIM setup	21
Figure 2.4: Rear of DIM	21
Figure 2.5: Front of DIM.....	22
Figure 2.6: DIM Dimensions	22
Figure 2.7: Close-up of segmentation mechanism in DIM.....	23
Figure 2.8: Model prep photos.....	25
Figure 2.9: Pressure gauge set up for pressure test of DIM	26
Figure 2.10: Pressure profiles from DIM and <i>in vivo</i> trial in upper jejunum.....	30
Figure 2.11: Recipient serum concentration of glucose.....	31
Figure 2.12: Summary of permeability results	32
Figure 3.1: DIM set up for increased gap between alternate contracting/relaxing ring pairs	40
Figure 3.2: SIM set up for increased gap between contracting and relaxing rings.....	40
Figure 3.3: Sections of DIM looked at for determining overall propagation.....	41

Figure 3.4: DIM during most of methylene blue trials.....	42
Figure 3.5: Permeability observed for given flow rates.	44
Figure 3.6: Time for methylene blue (MB) solution to advance through three different sections during flow rate trials.....	45
Figure 3.7: Permeability observed for given temperatures.....	47
Figure 3.8: Time for MB solution to advance through three different sections during temperature trials.....	47
Figure 3.9: Permeability observed for given viscosities	49
Figure 3.10: Time for MB solution to advance through three different sections during viscosity trials	50
Figure 3.11: Permeability observed given presence or absence of segmentation	52
Figure 3.12: Close up of DIM right after a contraction.....	53
Figure 3.13: Time for MB solution to advance through three different sections during segmentation trials.....	53
Figure 3.14: Permeability observed given particular orientation.....	55
Figure 3.15: Time for MB solution to advance through three different sections during orientation trials.....	55
Figure 3.16: Permeability observed for given segmentation placement.....	57
Figure 3.17: Time of MB solution to advance through three different sections during segmentation placement trials.....	57
Figure 3.18: Comparison of permeability values from <i>in vivo</i> trials and DIM trials.....	61
Figure 4.1: Components of digestive juices used	67
Figure 4.2: Diagram of the pre-intestinal phase of digestion trials	68
Figure 4.3: Digestion trial in DIM	71

Figure 4.4: Results of total glucose at each time point in digesta 73
Figure 4.5: Total glucose in DIM recipient serum..... 74
Figure 4.6: Total glucose results after 2h of digestion trials summarized 74

Chapter 1: Review of the Literature and Objectives

Pre-Intestine Digestion Overview

The gastrointestinal tract is a continuous tube that stretches from mouth to anus. Food is mixed with a variety of secretions that arise from both the gastrointestinal tract itself and organs accessory organs such as the liver, pancreas, and gall bladder. The intestine displays variety of motility patterns that serve to mix digesta with digestive secretions and move it along the length of the gastrointestinal tract (Barrett and others 2010).

The first act of mechanical digestion takes place in the mouth with the act of chewing. This is also where the first secretions to aid in digestion are encountered. These secretions are saliva from three glands that drain into oral cavity. This saliva has α -amylase to begin starch digestion but for the most part, saliva serves mainly to lubricate the food bolus with mucins to aid in the act of swallowing and transit down esophagus into the stomach (Barrett and others 2010).

In the stomach, the food is mixed with acid to lower the pH of digesta to around 2 in order to activate the pepsin used to breakdown protein in the food matrix. There are some lipases present in the stomach to break down larger fat molecules into smaller chained fatty acids but for the most part, protein digestion is what is accomplished in the stomach as well as further mechanical breakdown from the muscular organ. The digesta is then metered out into the duodenum through the pyloric valve. The time it takes to empty stomach contents depends primarily on the fat content of the meal (Barrett and others 2010).

Small Intestine Anatomy and Physiology

The small intestine is highly specialized for absorption of digested nutrients. Its irregular shape not only serves to pack so great a length into so small a cavity but it may also serve to help prolong digestion (Figure 1.1) (Barrett and others 2010). From Kararli (1995) review, it was shown that the lining the lumen of the small intestine are countless villi which are also lined with microvilli thus greatly increasing overall surface area for absorption to as much as 120 m² estimated absorbing surface area. These waves travel along the longitudinal muscle layer of the small intestine and propel digesta at an average flow rate of 10 mL/min; occasionally as fast as 20 mL/min (Fine and others 1995). Segmentation contractions persist as long as digesta is in the small intestine (Barrett and others 2010; Barron 1999; Sherwood 2011).

Various different enzymes are utilized throughout the entire digestive system for this purpose. Examples of these enzymes include pepsidases such as trypsin for protein breakdown and amylases responsible for breakdown of starch into glucose. In the small intestine, both the salivary and the pancreatic α -amylase also act on the ingested polysaccharides. Both the salivary and the pancreatic α -amylases hydrolyze 1:4 α linkages but spare 1:6 α linkages and terminal 1:4 α linkages. Consequently, end products of α -amylase digestion are oligosaccharides such as maltose and α -limit dextrans which are polymers of glucose containing an average of about eight glucose molecules with 1:6 α linkages. The oligosaccharides responsible for the further digestion of the starch derivatives are located in the brush border of small intestine (Figure 1.2). The effectiveness of the enzymes can be altered by inhibitors which work either on the enzyme itself or the substrate (Barrett and others 2010). Aside from the brush border enzymes, there are also pancreatic enzymes from the pancreas as well as bile from the

liver. Along with pancreatic lipases and amylases, the pancreas is also responsible of the secretion of HCO_3^- ions for raising the acidic pH of the digesta as it exits the stomach. The enzymes from the pancreas further breakdown the starches and fats in the digesta. The bile emulsifies said fat to make it easier for the pancreatic lipases to break them down. Pancreatic enzymes also include trypsins and chymotrypsins for further protein breakdown as well as ribonuclease and deoxyribonucleases for the breakdown of RNA and DNA respectively. Bile and pancreatic enzymes are secreted into the duodenum via the common bile duct (Barrett and others 2010).

One technique used to try and simulate digestion in the human small intestine is to utilize other animals such as rats, pigs, and chickens for *in vivo* digestion trials. Rats in particular are used a lot for studying the uptake of pharmaceuticals into the bloodstream from the intestines. With their smaller diameter and only an overall length of 92 cm, rat intestine is not very sufficient for human intestine simulation, especially when it comes to transit time (Willmann and others 2003). The actual length of the human intestine is roughly 2.8 m long. 25cm of that length is the duodenum. The remaining 260 cm of that being the jejunum and ileum combined (Table 1.1). Again though sources cited in a review by Kararli (1995) that puts total intestine at 6 m with both the jejunum and ileum measuring 300 cm each. This makes for a total transit time within the human small intestine on the order of 4 h (Barrett and others 2010). Roughly 7 to 145 s of that total transit time occur in the duodenum, the part of the small intestine where the digesta from the stomach is first mixed with bile and pancreatic enzymes. This was determined using magnetic markers. The wide ranging values were due to solid content, and thus viscosity of the digesta entering duodenum (Weitschies and others 1999). Kararli (1995) review cites that the transit time in the entire GI tract of humans,

not including colon, was actually unchanged by presence of food. It remained constant at around 20-30 h. However larger particles over 7 mm in size were withheld in the stomach longer but transit through the small intestine was fairly constant. Through permeability studies utilizing *in vivo* perfusion, theoretical pore sizes were calculated as a way of illustrating permeability of small intestine to nutrients. Permeability studies have shown the small intestine tends to vary, getting apparently smaller from the proximal to the distal end. Average theoretical pore sizes calculated ranged from 4 to 8 A, A for angstroms (Fordtran and others 1965; Fine and others 1995; Linnankoski and others 2010).

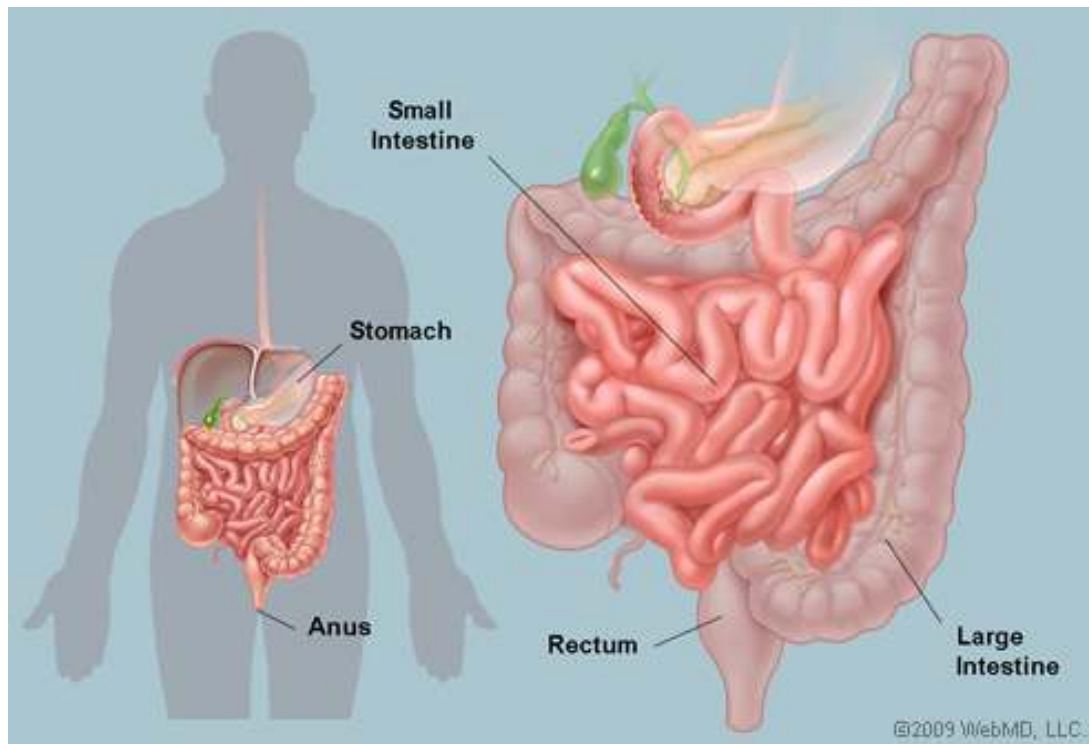


Figure 1.1: Small intestine anatomy. Note the many vertical and horizontal sections. Adapted from WebMD (2009).

Table 1.1: Digestive system average lengths. Adapted from Barrett and others (2010).

Segment	Length (cm)
Pharynx, esophagus, and stomach	65
Duodenum	25
Jejunum and ileum	260
Colon	110

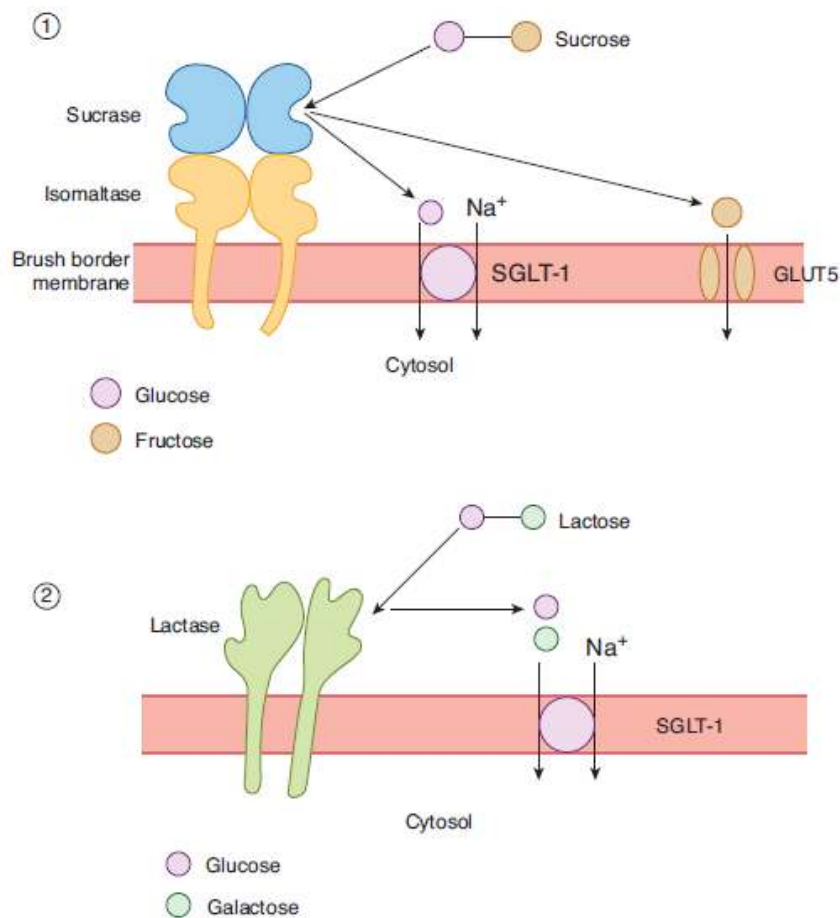


Figure 1.2: Brush border enzymes of small intestine. 1. Sucrase and Isomaltase. 2. Lactase. Adapted from Barrett and others (2010).

Dynamic Models for Simulating Intestinal Digestion

Dynamic small intestine models with physiologically similar characteristics are of increasing importance in food digestion studies aiming to develop healthy and functional food. One such model developed in the Netherlands is called TNO's gastrointestinal model (TIM) which makes use of varying water pressures to generate peristaltic motion in a flexible material contained in a glass jacket. This multiple compartment model simulates basic peristaltic motion of the gastrointestinal tract well and was used mainly in looking at viability of probiotics and not digestion kinetics and absorption (Yoo and Chen 2006) (Figure 1.3). The TIM model has its limitations. It neglects to model the diffusion of nutrients from digesta to a circulating recipient fluid that represents blood flow, opting instead to filter out the nutrients from digesta using hollow filter tubes (Yoo and Chen 2006). It has been used successfully in lipid bioaccessibility studies such as one involving conjugated linoleic acid-enriched milk and milk emulsions (Gervais and others 2009). Other models simulating nutrient absorption tend to use dialysis membrane such as a dialysis cell unit devised and tested by Savoie and Gauthier (1986), however the contents of dialysis cell were not subjected to any peristaltic motion such as in the TIM but instead agitated by a magnetic stir bar (Savoie and Gauthier 1986). Another dynamic model to consider is the Small Intestine Model (SIM) developed in the UK (Figure 1. 4). This model simulates the segmentation contractions seen in the small intestine (Tharakan and others 2010).

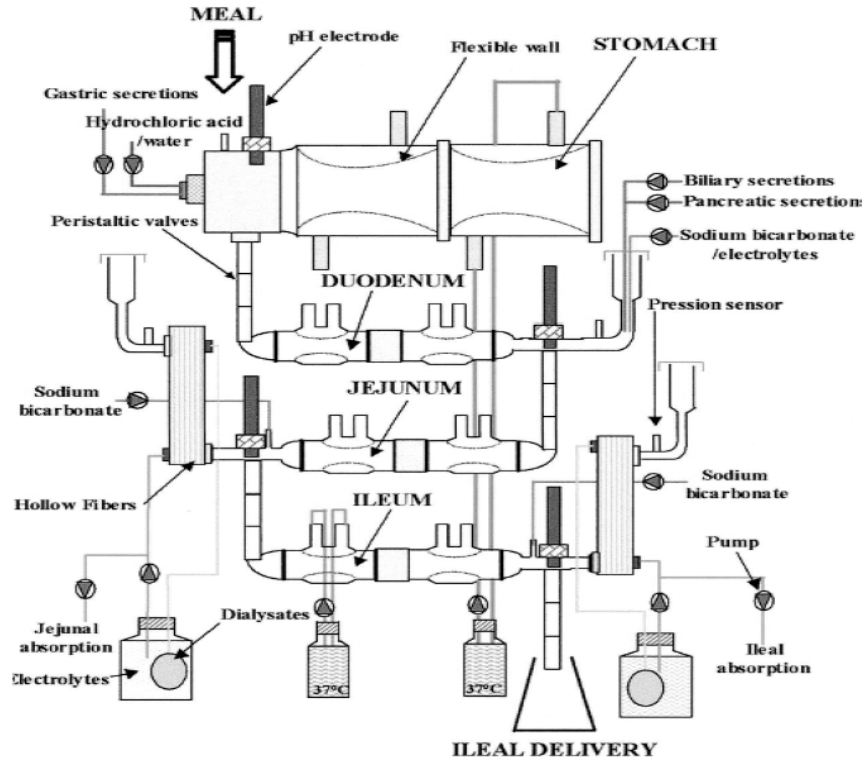


Figure 1.3: TIM model of stomach and small intestine. Adapted from Yoo and Chen (2006)

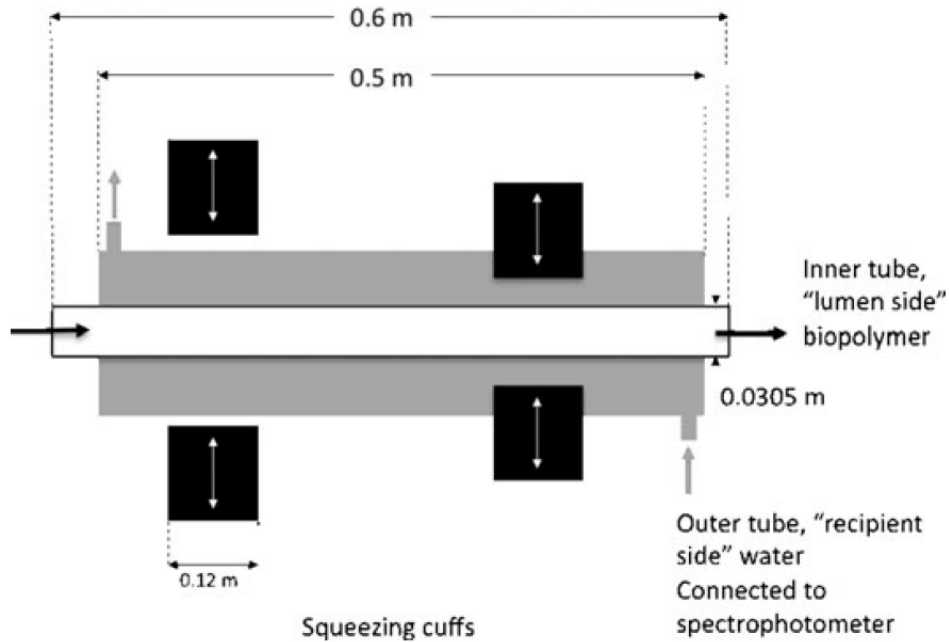


Figure 1.4: SIM segmentation schematic. Adapted from Tharakan and others (2010).

Digestion Kinetics

The mechanisms for nutrient absorption from the lumen of the intestine ultimately to the blood involve active as well as passive transport. Passive transport involves natural flow of solute with the concentration gradient meaning higher concentration to lower concentration. Active transport is the principle mode for absorption of amino acids and glucose (Barrett and others 2010; Tharakan 2008). This type of transport involves the expenditure of energy to move solutes against concentration gradient. As stated earlier, the passive transport or absorption of nutrients can be studied with *in vivo* perfusion of a segment of jejunum as was done by Fine and others (1995). From those studies, it was shown that changing the flow rate affected perceived permeability and thus theoretical pore size of intestine. Other factors have been found to effect absorption as well as forward propagation of digesta. Such factors include temperature and digesta viscosity. Temperature normally remains around 37°C with the intestines whereas the viscosity can vary from 0.01 all the way up to 10 Pa•s. The viscosity of the digesta tends to increase as it progresses through the small intestine as a good bit of water reuptake occurs within it (Barrett and others 2010). Study done by Tharakan and others (2008) illustrated how effective viscosity was in slowing the absorption of glucose using their SIM model described earlier. Flow rate also seems to affect perceived permeability but only up to a point (Fine and others 1995).

Enzyme Inhibition

Various different enzymes are used throughout entire digestive system for purpose of breaking down food into simpler and more readily absorbed macromolecules

such as glucose. Examples include peptidases such as trypsin for protein breakdown and amylases responsible for breakdown of starch into glucose. Effectiveness of the enzymes can be altered by inhibitors which work either on the enzyme itself or the substrate (Barrett and others 2010). Inhibition can occur by binding of the inhibitor with the substrate, preventing the enzyme to attach with the substrate and perform its function. This inhibition can be beneficial or detrimental depending on whether or not such effects are desirable or problematic. Examples of detrimental effects from enzyme inhibition include protein digestion inhibition in foods such as legumes. For the most part, these inhibitors can be deactivated by denaturing their protein structure with heat treatment, such as roasting (Zahnley 1984).

On the other hand, by inhibiting amylases, one would be inhibiting the breakdown of starch into glucose. This could prove beneficial to diabetics as blood sugar spikes would be less common and also reduced glucose uptake may help in weight loss attempts. One study looking at pine needle extract for example determined that use of such an extract greatly reduced glucose uptake and may exhibit α -glucosidase inhibitory characteristics but how exactly is not fully understood (Kim and others 2005). Other examples of beneficial starch inhibitors include aliphatic compounds, namely fatty acids as well as polyphenols including epicatechin-methylgallate and rutin (Takahama and Hirota 2010). This includes our own bile we produce in our liver and secrete into the duodenum to help aid in the digestion of fats. Studies have shown that bile can inhibit the digestion of buckwheat starch (Takahama and Hirota 2011).

Objectives of Study

This study aims to develop a Dynamic Intestinal Model (DIM). The importance of accurate *in vitro* models for digestion and absorption trials was the driving force for the

design of the Dynamic Intestinal Model (DIM) that will be tested and validated in the following three chapters of this thesis. Human *in vivo* trials have always been the best source of data for such trials but the high cost and at times ethical concerns can be daunting. The use of animal subjects have also brought their own ethical concerns along with the fact that the lab animals of choice for most pharmaceutical studies, the rat, has a GI tract vastly different when it comes to size and thus absorbable surface area.

From the information gathered, the DIM was developed and a couple of tests run for validation, including pressure and glucose absorption. Digestion kinetics were also studied using methylene blue to track propagation through the DIM and to further track absorption and thus perceived permeability of membrane. Finally a simple digestion trial using bread was run to look at actual starch digestion within the DIM and compare it to standing digestion trial using a shaking water bath. Also studied in this trial were the natural inhibitory effects of bile salts on starch digestion and how gastric digestion effects starch digestion.

References

- Barrett KE, Brooks HL, Boitano S, Barman SM. 2010. Section V Gastrointestinal Physiology. Ganong's Review of Medical Physiology 23rd Edition ed: McGraw Hill Medical. p. 429-87.
- Fine K, Santanna C, Porter J, Fordtran J. 1995. Effect of changing intestinal flow-rate on a measurement of intestinal permeability. *Gastroenterology* 108(4):983-9.
- Fordtran JS, Rector FC, Jr., Ewton MF, Soter N, Kinney J. 1965. Permeability characteristics of the human small intestine. *The Journal of Clinical Investigation* 44(12):1935-44.
- Kararli T. 1995. Comparison of the gastrointestinal anatomy, physiology, and biochemistry of humans and commonly used laboratory-animals. *Biopharmaceutics & Drug Disposition* 16(5):351-80.
- Kim Y, Jeong Y, Wang M, Lee W, Rhee H. 2005. Inhibitory effect of pine extract on alpha-glucosidase activity and postprandial hyperglycemia. *Nutrition* 21(6): 756-61.
- Larhed A, Artursson P, Grasjo J, Bjork E. 1997. Diffusion of drugs in native and purified gastrointestinal mucus. *Journal of Pharmaceutical Sciences* 86(6):660-5.
- Linnankoski J, Makela J, Palmgren J, Mauriala T, Vedin C, Ungell AL, Lazorova L, Artursson P, Urtti A, Yliperttula M. 2010. Paracellular Porosity and Pore Size of the Human Intestinal Epithelium in Tissue and Cell Culture Models. *Journal of Pharmaceutical Sciences* 99(4):2166-75.
- Sonavane G, Tomoda K, Sano A, Ohshima H, Terada H, Makino K. 2008. *In vitro* permeation of gold nanoparticles through rat skin and rat intestine: Effect of particle size. *Colloids and Surfaces B-Biointerfaces* 65(1):1-10.
- Takahama U, Hirota S. 2010. Fatty Acids, Epicatechin-Dimethylgallate, and Rutin Interact with Buckwheat Starch Inhibiting Its Digestion by Amylase: Implications for the Decrease in Glycemic Index by Buckwheat Flour. *Journal of Agricultural and Food Chemistry* 58(23):12431-9.

- Takahama U, Hirota S. 2011. Inhibition of Buckwheat Starch Digestion by the Formation of Starch/Bile Salt Complexes: Possibility of Its Occurrence in the Intestine. *Journal of Agricultural and Food Chemistry* 59(11):6277-83.
- Tharakan A. 2008. Modeling of physical and chemical processes in the small intestine. [Doctor of Engineering]. Birmingham, UK: The University of Birmingham. 286 p.
- Tharakan A, Norton IT, Fryer PJ, Bakalis S. 2010. Mass Transfer and Nutrient Absorption in a Simulated Model of Small Intestine. *Journal of Food Science* 75(6):E339-E46.
- Weitschies W, Cardini D, Karaus M, Trahms L, Semmler W. 1999. Magnetic marker monitoring of esophageal, gastric and duodenal transit of non-disintegrating capsules. *Pharmazie* 54(6):426-30.
- Willmann S, Schmitt W, Keldenich J, Dressman J. 2003. A Physiologic model for simulating gastrointestinal flow and drug absorption in rats. *Pharmaceutical Research* 20(11):1766-71.
- Yoo JY, Chen XD. 2006. GIT Physicochemical Modeling - A Critical Review. *International Journal of Food Engineering* 2(4).
- Zahnley J. 1984. Stability of enzyme-inhibitors and lectins in foods and the influence of specific binding interactions. *Advances in Experimental Medicine and Biology* 177:333-65.

CHAPTER 2
DYNAMIC INTESTINAL MODEL DEVELOPMENT AND PRESSURE
MEASUREMENT

¹ Wright, N.D. and Fanbin Kong. To be submitted to *Food Engineering*.

Abstract

Many food and drug studies would benefit from good simulations of digestion. By better understanding physiology of the human intestinal tract, better models could be developed to simulate digestion without having to resort to *in vivo* trials. The objective of this study was to develop a dynamic intestinal model (DIM) which, along with considering overall orientation and size, also looks at segmentation contractions found within the small intestine during the fed state. These contractions develop a regular pressure pattern with the intestines as seen in *in vivo* trials. The patterns generated by the DIM were similar to the pressure profile generated *in vivo* by other researchers using volunteer human subjects. It can be seen from these comparisons that DIM mimics the contractions in the small intestine. A permeability trial using a steady state concentration of glucose circulating within DIM was done to compare absorption characteristics in model to those of actual intestine.

Introduction

The small intestine is a key organ in the digestive system. It is here where the bulk of nutrient digestion and absorption takes place. The small intestine is highly specialized for nutrient absorption. Essentially a 5 cm diameter tube over 2.8 m long, it is packed tightly in the abdominal cavity producing many vertical and horizontal sections. Lining the lumen of the small intestine are countless villi which are also lined with microvilli thus greatly increasing overall surface area for absorption (Figure 2.1) (Kararli 1995). A slow flow rate of digesta through the intestinal lumen is important for

optimal absorption. Peristaltic waves triggered by pacemaker cells called interstitial cells of Cajal are responsible for forward propulsion of digesta. These waves travel along the longitudinal muscle layer of the small intestine and propel digesta at an average flow rate of 10 mL/min; occasionally as fast as 20 mL/min (Fine and others 1995). Flow rate is retarded by the action of segmentation contractions that are established in circular muscle layer. As the name implies, this contractions pinch off the intestine into segments each about 7 to 10 cm in length. The middle of each segment then constricts while the ends relax. This causes a back and forth mixing action on the digesta to help thoroughly mix it with digestive enzymes and bile as shown in Figure 2.2. This motion also slows down the flow of digesta, giving plenty of time for nutrient absorption (Barrett and others 2010). The time between contractions vary from one end of the small intestine on down to the other but it averages around a contraction every seven seconds. Segmentation contractions persist as long as digesta is in the small intestine (Barrett and others 2010; Barron 1999; Sherwood 2011).

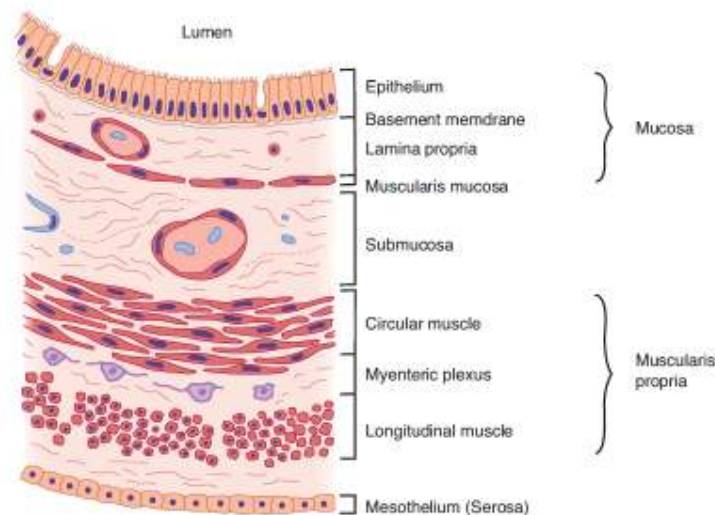


Figure 2.1: Organization of the wall of the intestine into functional layers. (Figure adapted from Barrett and others (2006)).

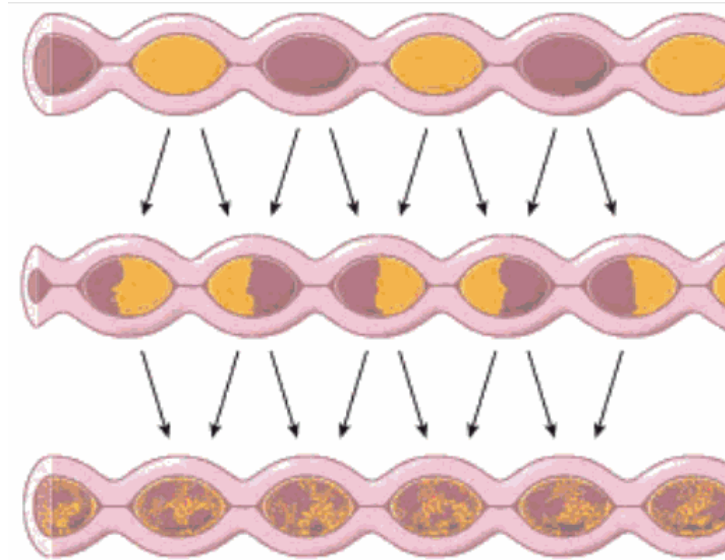


Figure 2.2: Mixing action of segmentation contractions. (Figure adapted from Sherwood (2011)).

It has become a major goal of researchers in the past couple of decades to develop gastrointestinal models that give reproducible results comparable to *in vivo* data. In terms of measuring digestion kinetics, the simplest approach involves the use of flasks or beakers with simulated meal and digestive juices in a shaking water bath (Hur and others 2009; Hur and others 2011). Greater interest has been placed on dynamic models that can better simulate the movements within the gastrointestinal tract. More and more advanced designs for gastrointestinal models have been developed as an alternative to *in vivo* studies. One example being the Gastric Human Simulator (HGS) developed by Kong and Singh (2010) which simulates very well the complex movements within the stomach responsible for mixing and size-reduction of food particles. This model took into account the shape and capacity of the actual human stomach (Kong and Singh 2010). Another model developed in the Netherlands is called TNO's gastrointestinal model (TIM) which makes use of varying water pressures to generate peristaltic motion in a flexible material contained in a glass jacket. This multiple

compartment model simulates the basic peristaltic motion of the gastrointestinal tract well and was used mainly in looking at viability of probiotics and not digestion kinetics and absorption (Yoo and Chen 2006). One of the main limitations of the TIM was that it neglects simulation of segmentation contractions that later dynamic models begin to focus more on, such as the SIM discussed a little later. The TIM model also neglects to model the diffusion of nutrients from digesta to a circulating recipient fluid that represents blood flow, opting instead to filter out the nutrients from digesta using hollow filter tubes (Yoo and Chen 2006). Other models simulating nutrient absorption tend to use dialysis membrane such as a dialysis cell unit devised and tested by Savoie and Gauthier (1986), however the contents of dialysis cell were not subjected to any peristaltic motion such as in the TIM but instead agitated by a magnetic stir bar (Savoie and Gauthier 1986).

Dynamic small intestine models with physiologically similar characteristics are of increasing importance in food digestion studies aiming to develop healthy and functional food. Aspects to look at for this kind of model would include segmentation contractions discussed earlier as well as a sigmoid design to represent the up and down segments of the small intestine. Segmentation contractions have been addressed with the Small Intestine Model (SIM) developed in the UK by Tharakan (2008). A dialysis membrane served as the inner tube immersed in a recipient fluid. Its contents however were mixed with the use of peristaltic motion via pumps and segmentation contractions with the use of blood pressure cuffs (Tharakan and others 2010). One big disadvantage with this model is that it was run at room temperature only. Another concern was its segmentation mechanism. The blood pressure cuffs used not only contracted the inner

membrane but the flexible outer membrane as well. It could be hypothesized that this approach could inhibit the diffusion of nutrients or pharmaceuticals from the inner membrane into recipient fluid circulating in outer membrane. The main body of SIM is a horizontal tube, which is different from the actual shape of human intestine which contains many ascending and descending sections. We hypothesize the sigmoidal shape of intestine may have important function in keeping large particulates for longer retention time for more complete digestion. The aim of this study is to develop a more comprehensive dynamic small intestine model. The model will incorporate realistic simulation of segmentation motion and the irregular shape. To validate the model, the pressure profile generated within the model intestinal tract was measured and compared with intestinal pressure obtained by *in vivo* trials done by Samsom and others (1999). The permeability of glucose was also studied with the model and those results were compared with *in vivo* results obtained by Fine and others (1995).

Model Development

This Dynamic Intestinal Model (DIM) was made from two halves of a machined acrylic block. Machined in these halves were sigmoid-shaped grooves that, when the halves were joined, formed a sigmoid cylinder that contained circulating recipient fluid. Within this cylinder were placed contraction rings and dialysis membrane. The membrane tube acted as the intestinal tract. There were also a couple of low capacity peristaltic pumps used for digesta and enzymes as well as a larger capacity one for recipient fluid circulation. Said recipient fluid was heated within water bath to help maintain physiological temperature conditions, i.e 37°C. Details of all components are discussed in the following sections, and also shown in figures 2.3-2.7.

Main Body

The main body of the model consists of two halves of an acrylic block 10 cm high and 15 cm long (Figure 2.3). A sigmoid groove 2.6 cm deep was machined in the two halves along with a smaller groove for an o-ring seal and screw holes. The two halves formed a water-tight sigmoid cylinder joined together. This cylinder had a diameter of 5.2 cm and an overall length of roughly 57 cm. Within this cylinder were set 10 contraction rings which will be detailed in the next section. A 59 cm section of dialysis membrane tubing (Spectra/Por 7, 8000MWCO; Spectrum Laboratories Inc.; Santa Dominguez, CA) was threaded through these rings and secured by two acrylic block caps at the entrance and exit of the sigmoid cylinder. Rubber stoppers placed in these blocks held the membrane and also served as a port for tubes to fill the membrane and to remove digesta. A larger sampling point/pressure port was also placed in the top stopper. This main body was secured to a stainless steel stand.

Contraction Rings and Controls

To simulate the segmentation contractions found in the small intestine, 10 stainless steel contraction rings were made. These rings and the support stem that was secured to the back half of the main body were hollow with six raised openings around the inside of each ring (Figure 2.7). On these raised openings were attached rubber finger cots. During operation of the model, half of the rings would have air supplied to them at 2.5 psi and the other half would have a vacuum applied. This pattern of contraction would alternate once every 7 s as determined by programmable logic control mounted on the back of the model. The control operated a valve that switched

air/vacuum between the rings. Also housed behind the model was a regulator for the air and a bypass placed after the regulator so that vacuum could be applied to all rings to make loading of membrane easier. Vacuum source was the vacuum outlet in the lab while air was supplied by a tank.

Pumps for Digesta, Enzyme Secretion, and Recipient Fluid:

Two separate low capacity peristaltic pumps (FH10 Microflex, Thermo Scientific Inc., Barrington, IL) were utilized for the movement of digesta and enzymes respectively into the model. Tubes from both pumps were joined by a t- connector to one tube that was attached to the inlet post of the entrance stopper for membrane tube. Larger tubing attached to ports in the back of the block caps were used to fill the sigmoid cylinder and circulate recipient fluid through it and around the dialysis membrane tube. A large capacity peristaltic pump (Easy-Load HV-77601-10, Cole-Parmer Inc., Vernon Hills, IL) capable of speeds up to 600 rpm was used for this purpose. This also served as part of the temperature control system. The beaker containing the recipient fluid of choice was placed in a water bath (89032-204, VWR International Inc., Radnor, PA) set to the desired temperature of 37°C.

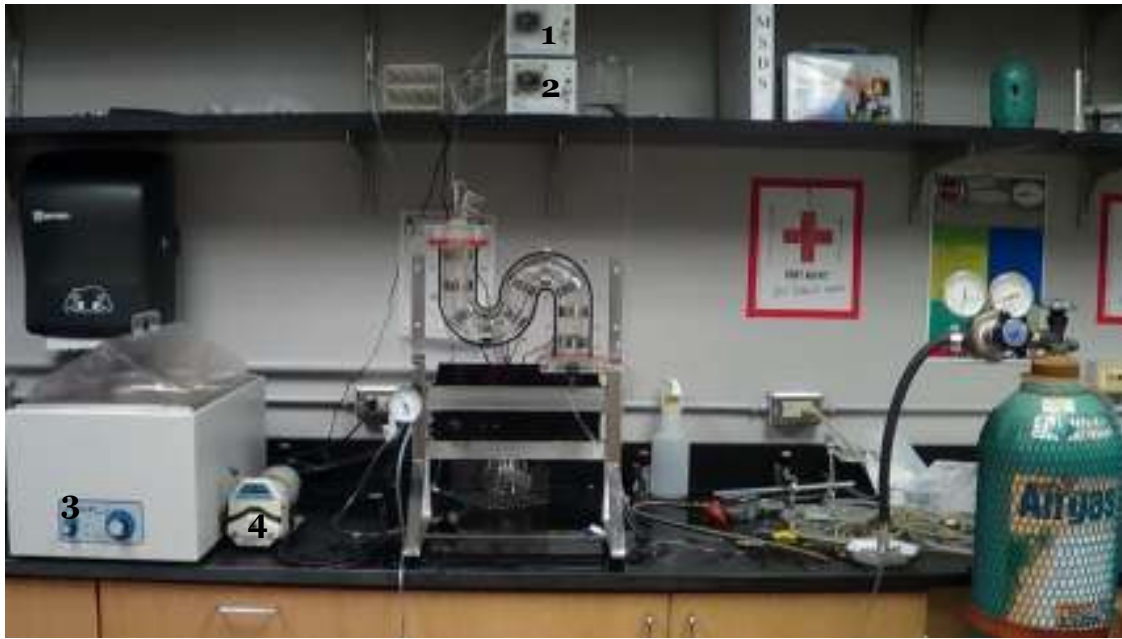


Figure 2.3: Overall view of DIM setup. 1. Thermo Scientific peristaltic pump used for digesta. 2. Thermo Scientific FH10 pump for duodenal/bile juice. 3. VWR water bath for heating recipient fluid. 4. Masterflex Easy-Load Pump for circulating recipient fluid.

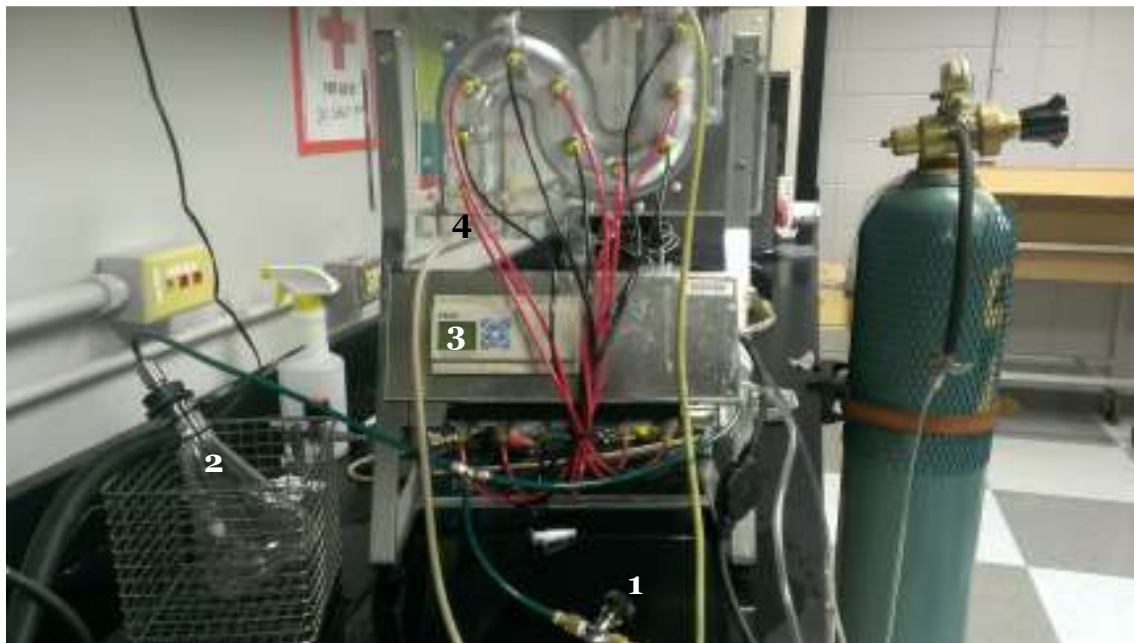


Figure 2.4: Rear of DIM. 1. Bypass valve. 2. Vacuum Trap (to prevent liquid from accidentally entering vacuum system). 3. Programmable logic for setting rate of contractions. 4. Recipient fluid inlet. 5. Recipient fluid outlet. Also visible is the air supply.

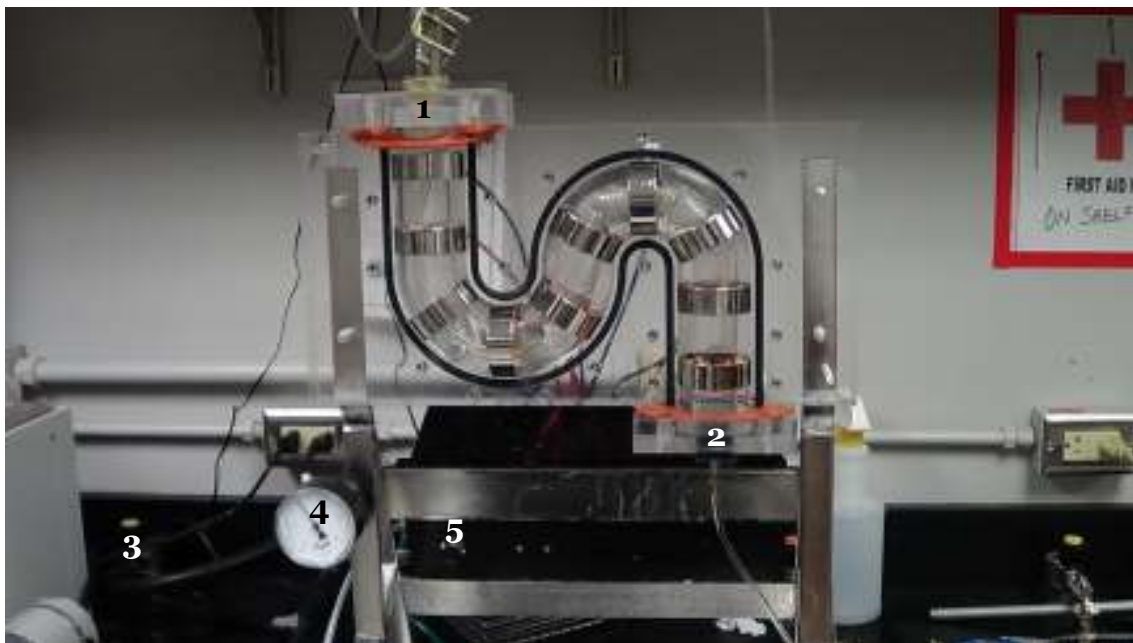


Figure 2.5: Front of DIM (front cover removed for clear view of membrane and rings). 1. Top/entrance block with stopper, digesta/enzyme inlet tube (small diameter), and sampling tube (larger diameter) with metal clamp. 2. Bottom/exit block with stopper and fill/outlet tube. 3. Vacuum source. 4. Pressure gauge. 5. Pressure regulator.

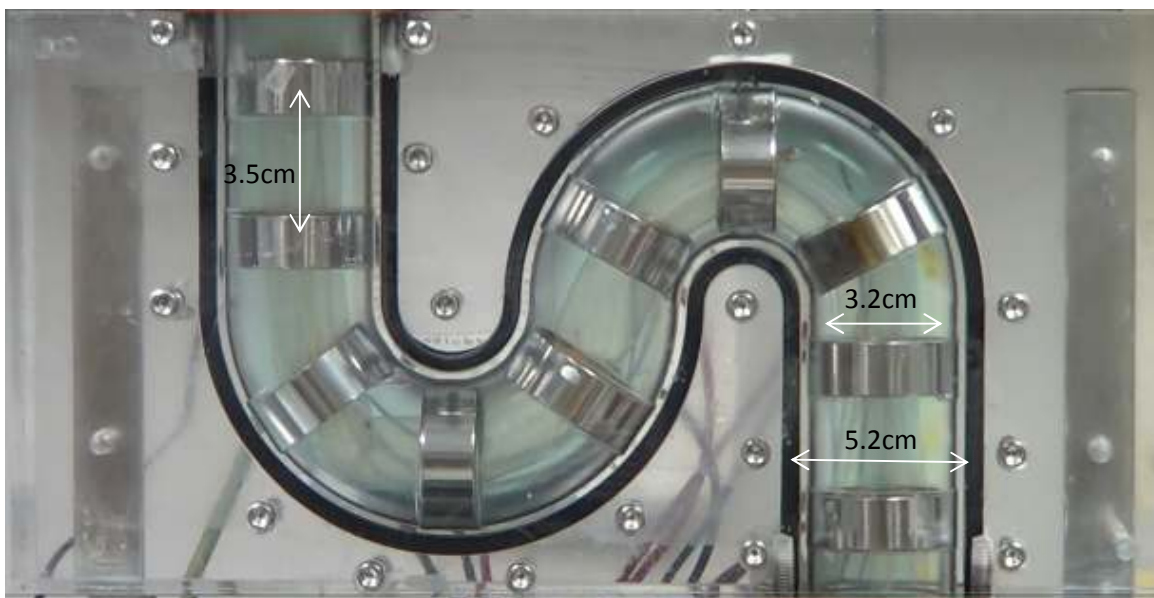


Figure 2.6: DIM dimensions. The 3.5cm is the space between rings. 3.2cm is diameter of inner membrane. 5.2cm is diameter of outer, recipient tube.



Figure 2.7: Close-up of segmentation mechanism in DIM. These rings can contract to a diameter of roughly 1 cm. Inner diameter of contraction rings is 3.5 cm.

Protocol of DIM Operation:

Before a trial is run, it is necessary to prep the model. There are 3 basic steps: loading and filling membrane, securing front, removable acrylic model half, and filling the outer annular space surrounding the filled membrane. Prep usually takes no longer than 5-10min to complete. All the prep steps were illustrated in Figure 2.8. First the valve for the vacuum was opened (I). The next step was to open the bypass valve so that the vacuum could be applied to all segmentation rings. This makes for easier loading of the membrane (II). Now the bottom black cork was inserted carefully into the membrane so as not to tear it (III). Membrane and stopper was then inserted into bottom end block and membrane carefully threaded through the contraction rings (IV). The open end of the fill tube was then placed into a beaker of deionized water and then

drawn out once partially filled to fill the membrane by gravity. Tube clamp was used as a weight to keep fill tube in place (V). Membrane was allowed to fill to the middle of the left most section of model and then the model was carefully tilted a little over 90° clockwise to clear air bubble from top middle section (VI). The top stopper with the inlet port for draw tube and the sampling/collection was then inserted in the membrane and the draw tube was attached after filling membrane to just above the first contraction ring VII. The filling of membrane resumed until water was visible in the draw tubing. The tubing was then placed in the peristaltic pumps; one for digesta and one for enzyme mix, and tubes were primed, removing all air (VIII). At this point membrane was firm and water inside slightly under pressure. This was a good time to check for any leaks. None were found, so the outer acrylic cover was placed over the rings and the inner acrylic block and secured with screws (IX). Bypass valve was closed and air flow from tank to the model was opened. Regulator on air tank was opened slowly at first to equalize the pressure gently to 2.5 psi, the set pressure on the model's regulator. Once this pressure was reached, the regulator on the air tank was opened further to 40 psi. This was the operating pressure used for the pneumatically driven valve that alternates air/vacuum to the 10 contraction rings (X). The annular space of the model was then filled with deionized water using high flow peristaltic pump. A total of 1 L of water was circulated within the model's annular space. Segmentation mechanism was then turned on after about half of the annular space was filled to clear any air bubbles stuck to the finger cots that were in the vacuum state. Rings were allowed to go through a couple of cycles. Air relief valve located in back of model behind top curve of model (indicated in photo IX in Figure 2.8) was then closed once annular space was full.

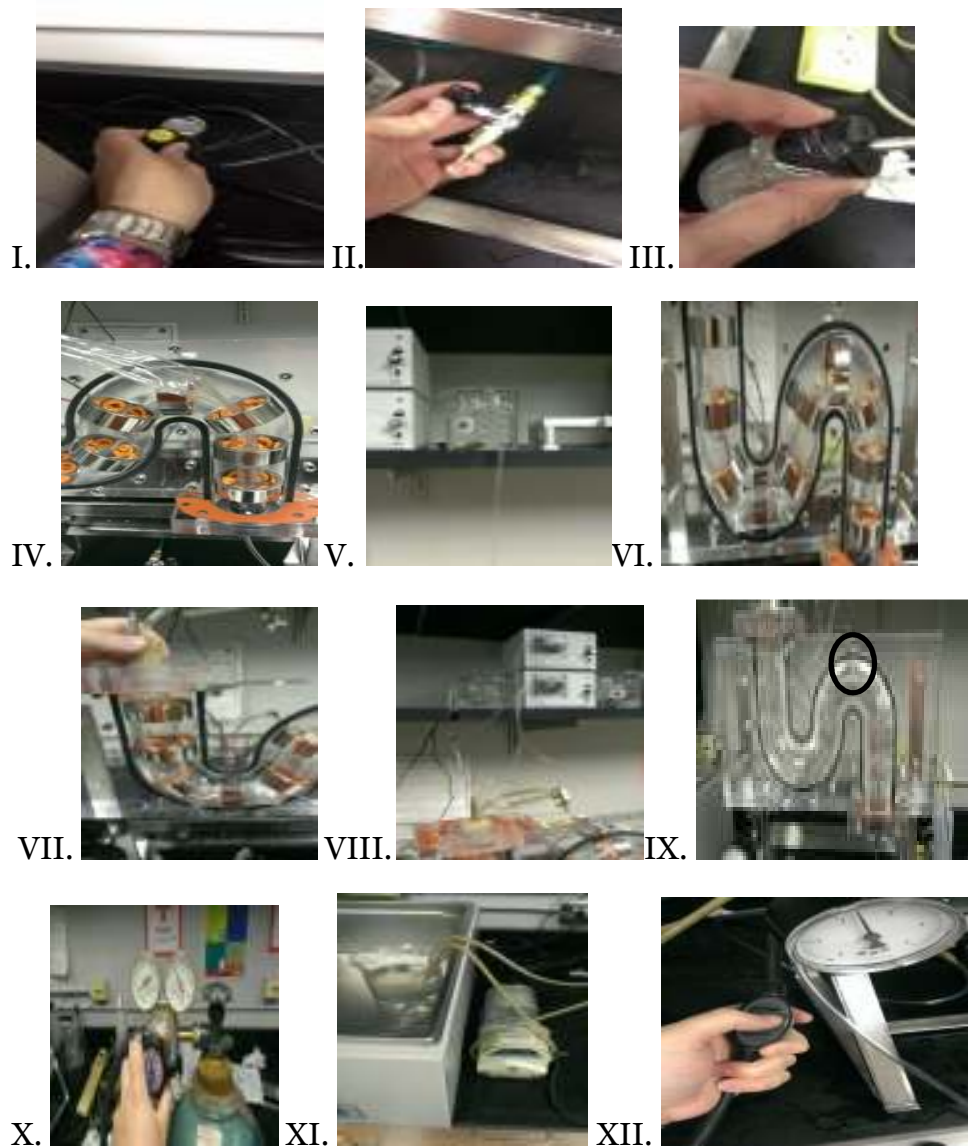


Figure 2.8: Model prep photos. Steps outlined in full detail above.

Materials and Methods

Pressure Test

To measure pressure within the model, the sample tube placed within the membrane via the top stopper was attached to another plastic tube that attached to a digital pressure meter. Care was taken to ensure that the tube was completely sealed so

that when the membrane was filled, an air cushion would form within the tube. This column of air would thus compress or expand depending on the pressure exerted on it by the membrane contents. For this trial, the procedures described above were followed but after the front block was secured, the pressure was allowed to equilibrate at the flow rate of 10 mL/min. Once that was done, the contractions were started and pressure gauge recorded to view pressure changes with contractions. This was done for duration of 1 min.

For pressure profile measurements, a digital pressure gauge (Model 2074, Ashcroft Inc., Stratford, CT) was used with units set at kPa (Figure 2.9). This gauge was attached to a plastic, open-ended tube inserted and sealed into the inside of the membrane tube. Two different conditions were looked at in this study. One profile was generated in the DIM with all 10 rings while another profile was generated with just 5 of the rings. Pressure profiles were manually plotted every second for 1min in a spreadsheet and compared with pressure profiles from studies done by Samson and others (1999). Readings were taken from pressure gauge recorded with a digital camcorder (HDR-CX220/B, Sony Electronics Inc., Tokyo, Japan) every 1 s.



Figure 2.9: Pressure gauge set up for pressure test of DIM. Note units set for kPa.

Glucose Permeability

Permeability trial was run using glucose in a steady state condition. A 300 mg/dL glucose solution was made by dissolving 1.5 g of glucose in 500 mL of DI water. A UV/Vis spectrophotometer (Evolution 300, Thermo Scientific Inc., Barrington, IL) was used for all concentration measurements by utilizing the DNS method. For this method a solution of dinitrosalicylic acid was made as outlined by Miller (1959) with slight modifications. Standard curve was made from absorbance values of solutions with known glucose concentration. Glucose was used as it is much closer to the molecular weights of the test solutes used in study by Fine and others (1995). Prepping of the DIM was carried out as described in the model protocol section earlier with the glucose solution being used to fill the membrane and prime the tubes instead of DI water. Once the model was prepped, the beaker with remaining glucose solution, roughly 250 mL after air was applied to half the segmentation rings and the recipient fluid began circulating, was moved over by the digesta and enzyme pumps. Both inlet tubes were placed in the beaker along with the fill/outlet tube and the pumps adjusted to a steady circulation rate of 10mL/min. Thus the glucose solution was circulated through the membrane for the entire trial. Aliquots of 1.5 mL were taken from the recipient fluid beaker within the 37°C water bath every 5 min for 20min resulting in 15 samples taken overall, including a time zero sample. Again all samples were taken in triplicate. 1 mL of DNS was added to each sample and heated in a boiling water bath for 15 min followed by rapid cooling to room temperature in ice water. The samples were then diluted with 8 mL of DI water and read on the UV/Vis spectrophotometer at 576 nm to get glucose concentration (Miller 1959). The permeability of membrane was derived using

techniques from study done by Fine and others (1995). This study involved the perfusion of test solute in non-absorbable polyethylene glycol (PEG) into a 30cm segment of jejunum in live volunteers. They estimated permeability by taking the observed absorption rate J and dividing it by the observed concentration gradient ΔC . This gives a unit of permeability as $J/\Delta C$. These were used in the glucose trial along with a conversion factor of 0.6333. This was needed to convert units in DIM trials to units used trial done by Fine and others (1995). Conversion factor was calculated from equation 1.

$$\frac{L}{57cm \cdot 20min} \times \frac{57cm \cdot 20min}{30cm \cdot 60min} \times \frac{60min}{h} = \frac{L}{57cm \cdot 20min} \times 0.6333 = \frac{L}{30cm \cdot h} \quad (\text{Eq.1})$$

Results and Discussion

Pressure Test

Pressure profiles were generated within DIM from segmentation contractions. The DIM displayed more regular contraction patterns than those obtained *in vivo* and pressure spikes were closer in magnitude between *in vivo* results done by Samsom and others (1999) and DIM results utilizing all 10 segmentation rings. It was unexpected to observe more high peaks when half the contraction rings were in use as opposed to all 10. This may be due to the fact that the pressure equalizes more slowly when fewer rings are used and thus the high peaks were seen on the gauge with greater ease. Pressure changes using the digital gauge were subject to instantaneous peaks and quicker decay after the contraction cycle had ceased. *In vivo* pressure profiles in the upper jejunum have been studied using novel manometer devices inserted trans-nasally into volunteer

subjects (Samsom and others 1999) to look primarily at the propagation of propulsion waves in the intestine. From that study, good pressure profile data was gathered after subjects completed a lunch meal. One of those profiles were scaled up and compared to the data derived from the pressure tests performed on the DIM (Figure 2.10). Similar profiles were observed between the DIM and *in vivo* trials even with altering the number and location of segmentation contractions within the DIM.

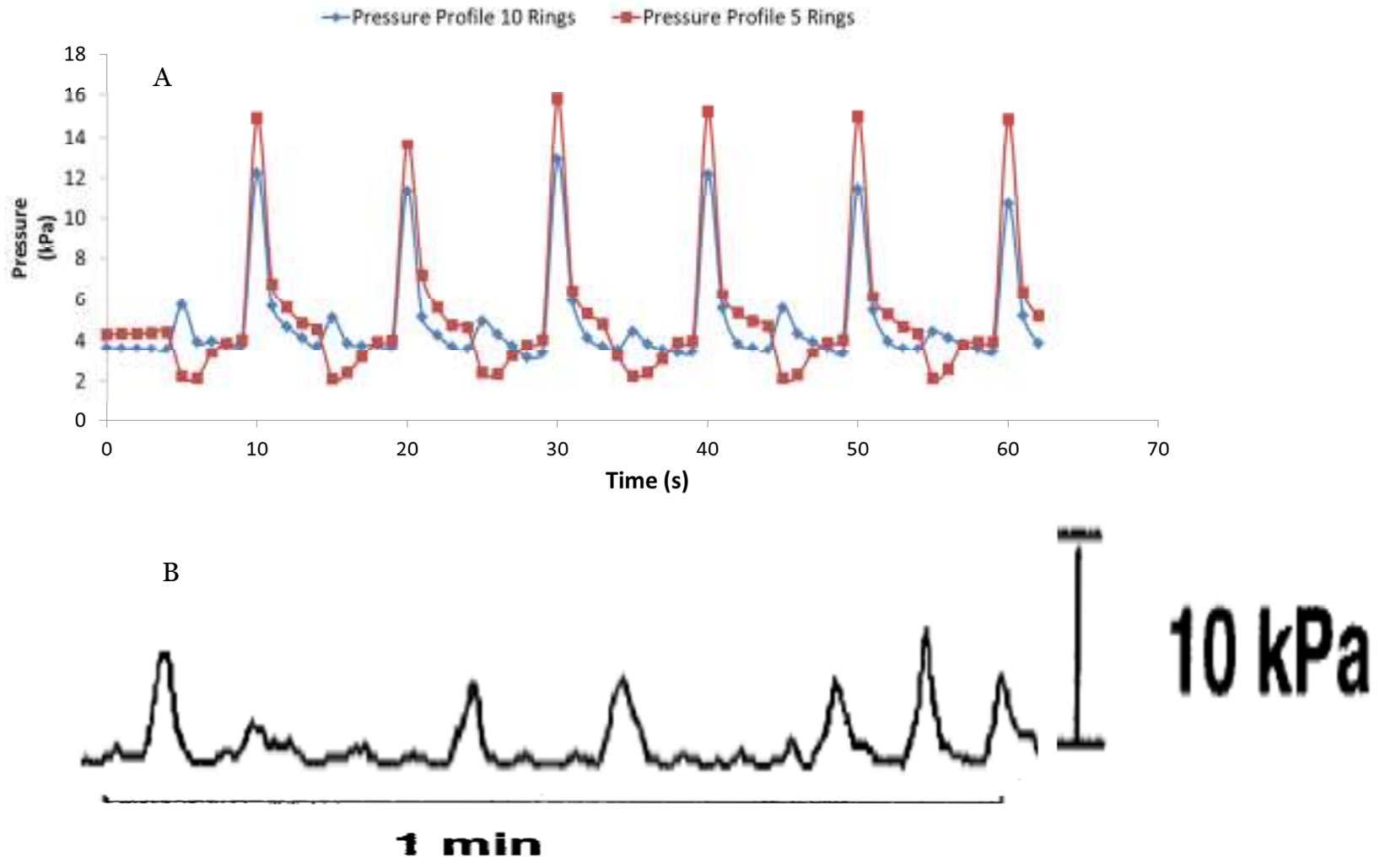


Figure 2.10: Pressure profiles from DIM (A) and *in vivo* trial in upper jejunum done by Samsom and others (1999). Both represent 1 min of data.

Glucose Permeability

The results of glucose concentration in recipient fluid are shown in Figure 2.11 below. With flow rate of 10 mL/min, 0.001Pa·s viscosity and 37°C temperature, the calculated permeability value for the DIM membrane was $3.469 \times 10^{-2} \text{L}/30\text{cm}\cdot\text{h}$. The results were compared with the *in vivo* data from Fine and others (1995). The calculated permeability for the DIM membrane using glucose is similar to the $3.000 \times 10^{-2} \text{L}/30\text{cm}\cdot\text{h}$ found for mannitol used in Samsom and others (1995) *in vivo* study. Figure 2.12 indicates that glucose permeability value is close to mannitol, which is expected as glucose has a lower molecular weight than mannitol. Glucose was used though in the DIM model because of the ease to measure its concentration with DNS method.

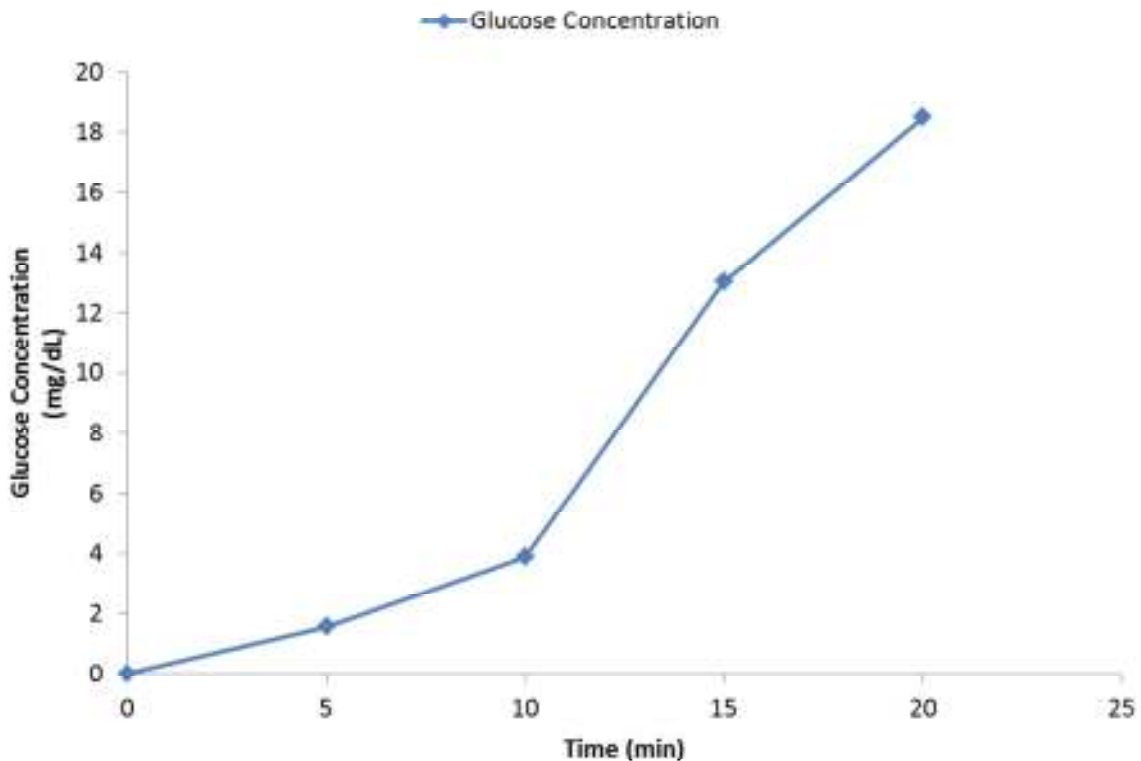


Figure 2.11: Recipient serum concentration of glucose per time. Concentration gradients generated from the data above were used to figure glucose permeability.

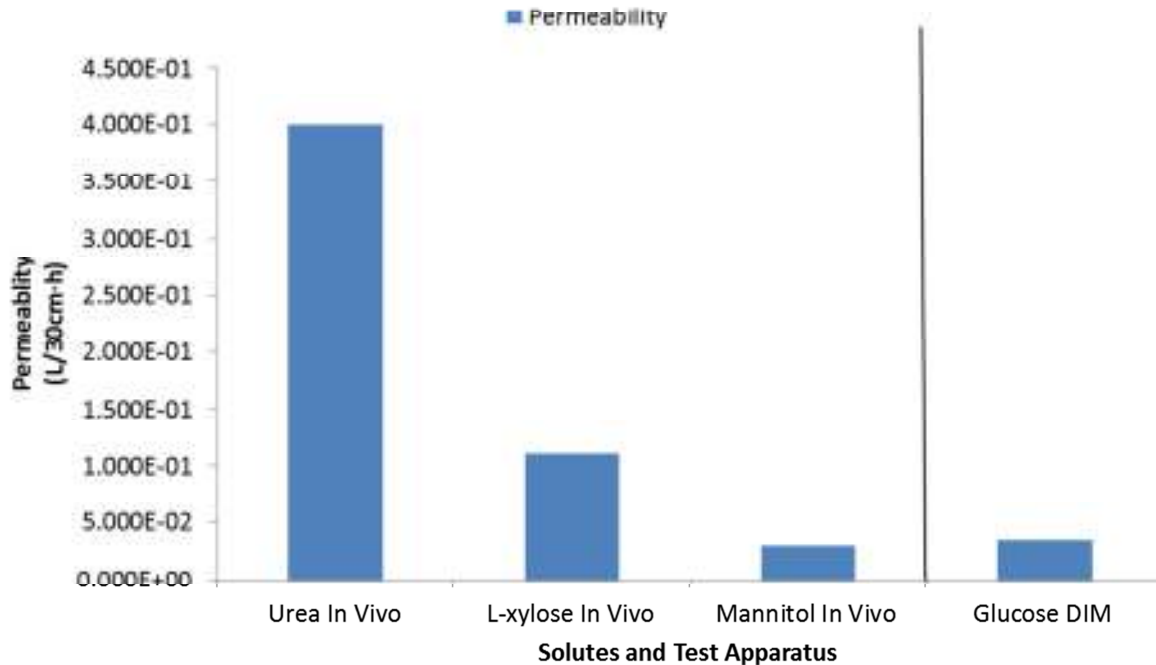


Figure 2.12: Summary of permeability results from Fine and others 1995 study and glucose permeability trial in DIM.

Conclusions

The DIM was developed as a robust *in vitro* digestion tool as a means to accurately run digestion trials without having to resort to *in vivo* trials. In particular, with its length being over 50cm, the DIM could represent the human duodenum, at 25cm, and part of the jejunum. The DIM incorporates realistic simulation of sedimentation and orientation to improve accuracy of digestion simulations. The segmentation contractions that occur within the small intestine are to help thoroughly mix digesta with enzymes. The pressure profiles generated within the DIM shows great similarities with the pressure profiles obtained with *in vivo* trials.

By performing an absorption trial with glucose solution, permeability values for the membrane used in the DIM were calculated. These values were then compared to

perfusion studies done *in vivo* and values found for permeability were in good agreement, especially when comparing the mannitol *in vivo* data with the glucose DIM data.

References

- Barrett KE, Brooks HL, Boitano S, Barman SM. 2010. Section V Gastrointestinal physiology. Ganong's Review of Medical Physiology 23rd Edition ed: McGraw Hill Medical. p. 429-87.
- Barron John Physiology of the Small Intestine, Part.1. 1999 [Accessed 2012 May, 24] <http://www.jonbarron.org/article/physiology-small-intestine-part-1>.
- Fine K, Santanna C, Porter J, Fordtran J. 1995. Effect of changing intestinal flow-rate on a measurement of intestinal permeability. Gastroenterology 108(4):983-9.
- Hur S, Decker E, McClements D. 2009. Influence of initial emulsifier type on microstructural changes occurring in emulsified lipids during *in vitro* digestion. Food Chemistry 114(1):253-62.
- Hur SJ, Lim BO, Decker EA, McClements DJ. 2011. *In vitro* human digestion models for food applications. Food Chemistry 125(1):1-12.
- Kararli T. 1995. Comparison of the gastrointestinal anatomy, physiology, and biochemistry of humans and commonly used laboratory-animals. Biopharmaceutics & Drug Disposition 16(5):351-80.
- Ganong's Review of Medical Physiology 23rd Edition ed: McGraw Hill Medical. p. 429-87.
- Miller GL. 1959. Use of dinitrosalicylic acid reagent for determination of reducing sugar. Analytical Chemistry 31(3):426-8.
- Kong FB, Singh RP. 2010. A Human Gastric Simulator (HGS) to Study Food Digestion in Human Stomach. Journal of Food Science 75(9):E627-E35.
- Sansom M, Fraser R, Smout A, Verhagen M, Adachi K, Horowitz M, Dent J. 1999. Characterization of small intestinal pressure waves in ambulant subjects recorded with a novel portable manometric system. Digestive Diseases and Sciences 44(11):2157-64.
- Savoie L, Gauthier SF. 1986. Dialysis Cell for the *In Vitro* Measurement of Protein Digestibility. Journal of Food Science 51(2):494-8.
- Sherwood L. 2011. Fundamentals of Human Physiology: Cengage Learning.
- Tharakan A, Norton IT, Fryer PJ, Bakalis S. 2010. Mass Transfer and Nutrient Absorption in a Simulated Model of Small Intestine. Journal of Food Science 75(6):E339-E46.

Yoo JY, Chen XD. 2006. GIT Physicochemical Modeling - A Critical Review.
International Journal of Food Engineering 2(4).

CHAPTER 3
PERMEABILITY AND PROPAGATION PATTERNS OF METHELYNE BLUE
IN DYNAMIC INTESTINAL MODEL (DIM)

¹ Wright, N.D. and Fanbin Kong. To be submitted to *Food Engineering*.

Abstract

An important attribute of the human digestive system to consider includes its ability to take in simple nutrients once they're broken down by digestion. Active transport against the concentration gradient at the expense of energy is common in small intestine but passive diffusion does occur as well. In this chapter, similar trials with DIM using methylene blue as solute were conducted to assess permeability values, as well as the propagation rates. The movement of the methylene blue was observed as an indicator of mixing action and turbulent flows that accompany the segmentation contractions. Several different factors were tested including temperatures of 26, 32, 37, and 42°C; viscosity of 0.001, 1.27, 2.13, and 6.01 Pa·s; flow rates of 5, 10, and 15 mL/min; orientation, and segmentation placement on the permeability of DIM membrane as well as propagation of digesta through the model. Results showed expected diffusion behavior base on Stokes-Einstein equation effecting both forward propagation of digesta and permeability of membrane observed.

Introduction

The mechanisms for nutrient absorption from the lumen of the intestine ultimately to the blood involve active as well as passive transport. Passive transport involves natural flow of solute with the concentration gradient meaning higher concentration to lower concentration. Active transport is the principle mode for absorption of amino acids and glucose (Barrett and others 2010; Tharakan 2008). This type of transport involves the expenditure of energy to move solutes against concentration gradient. Despite this fact, *in vivo* studies have provided strong theoretical data for pore size (Fine and others 1995; Linnankoski and others 2010; Fordtran and others 1965) as well as permeability of intestinal tissue (Larhed and others

1997; Sonavane and others 2008). Studies by Fine and others (1995) showed that changing the flow rate affected perceived permeability and thus theoretical pore size of intestine. Temperature and viscosity have been shown to effect both propagation and perceived permeability. By increasing temperature, both parameters increase while the inverse is seen with viscosity. With increasing viscosity, propagation rate and perceived permeability decreased (Ellis and others 1995; Larhed and others 1997; Linnankoski and others 2010). This data was used to validate intestinal models that make use of dialysis membranes such as the SIM model developed in Britain (Tharakan and others 2010).

The purpose of the research described herein was to determine propagation rate of intestinal contents and the permeability of nutrients through membrane wall of intestine. For this purpose, a methylene blue solution was utilized. Methylene blue was chosen for its comparative molecular weight, 319 g/mol, to glucose, 181 g/mol, as well ease of detection even at small concentration using UV/Vis Spectrophotometry. Methylene blue also served as an ideal visual indicator of the mixing pattern caused by the simulated segmentation contractions as well as overall forward propagation.

Materials and Methods

For the permeability trials, 2 L of 500 ppm Methylene blue solution was prepared by dissolving 1g of Methylene blue in 2 L of DI water. Methylene blue was chosen for these trials due to its ease of detection using UV/Vis spectrophotometry as well as its visibility through the acrylic which assisted in tracking mixing patterns and overall forward propulsion. A beaker of 500 mL of 500 ppm methylene blue was used for each trial. Primary temperature control was achieved with the circulating recipient fluid. Different factors looked at during the trials were the effects of flow rate, temperature,

and viscosity of solution as well as model orientation, presence or absence of segmentation, and segmentation placement on the permeability of membrane representing intestinal wall, and the propagation rates of methylene blue in the intestine.

The overall method for each trial was similar. The DIM membrane (Spectra/Por 7, 8000 MWCO; Spectrum Laboratories Inc.; Santa Dominguez, CA) was filled with DI water according to the operation protocol described before. Then methylene blue solution is pumped into the tube. All trials were run for 20 minutes, until the methylene blue reached the end of the intestinal tube. 1.5 mL aliquots were taken in triplicate every 5 minutes from the circulating recipient fluid which for these trials was deionized water. With the flow rate trials, the two peristaltic pumps (FH10 Microflex, Thermo Scientific Inc., Barrington, IL) were set to maintain flow of 5 mL/min, 10 mL/min, and 15 mL/min respectively. These trials were done at room temperature of 26°C. For the temperature trials, three temperatures 32, 37, and 42°C were used. All the trials to follow were run at flow rate of 10 mL/min and temperature of 37°C. For the viscosity trials, three different guar gum concentrations 0.05, 0.1, and 0.2% were used. Viscosity measurements were done using a rheometer (902-00138, Rheometric Scientific, Inc., Piscataway, NJ) using 1" parallel plate set up. Viscosity measurements were done at 37°C since that was the temperature at which the viscosity trials were run. The percentage of guar gum used in the trials represented viscosities of 0.001, 1.27, 2.13, and 6.01 Pa·s respectively. A trial was run with no segmentation. Effect of orientation was also studied by running a trial with the model turned 90° clockwise. Finally a couple of trials with different placement of the segmentation rings were done. One trial looked at spreading the gap between pairs of contracting/relaxing rings and the other looked at

widening gap between contracting and relaxing rings. Both conditions illustrated below in Figures 3.1 and 3.2.

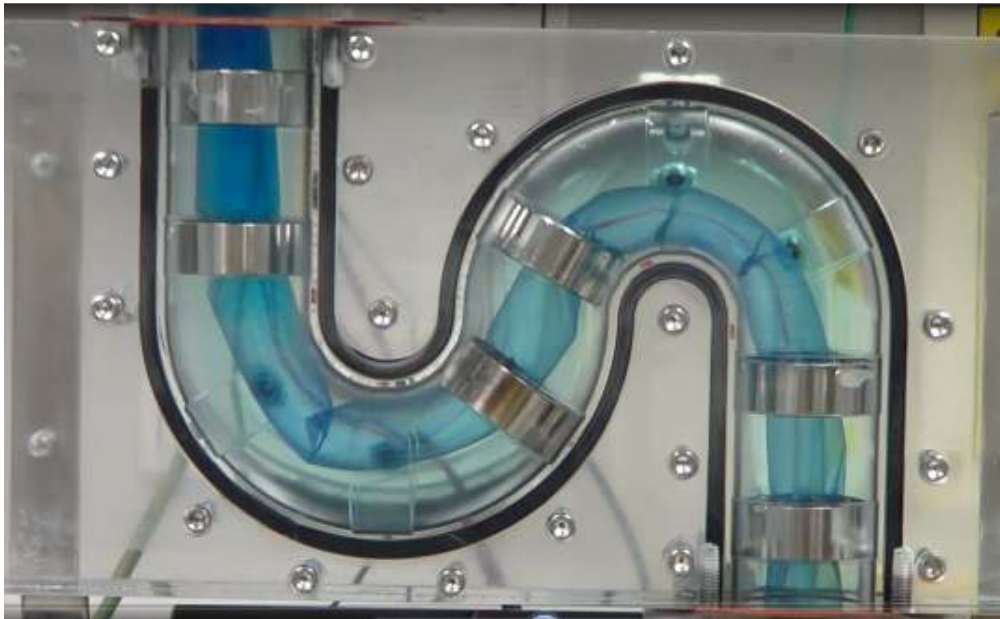


Figure 3.1: DIM set up for increased gap between alternate contracting/relaxing ring pairs.

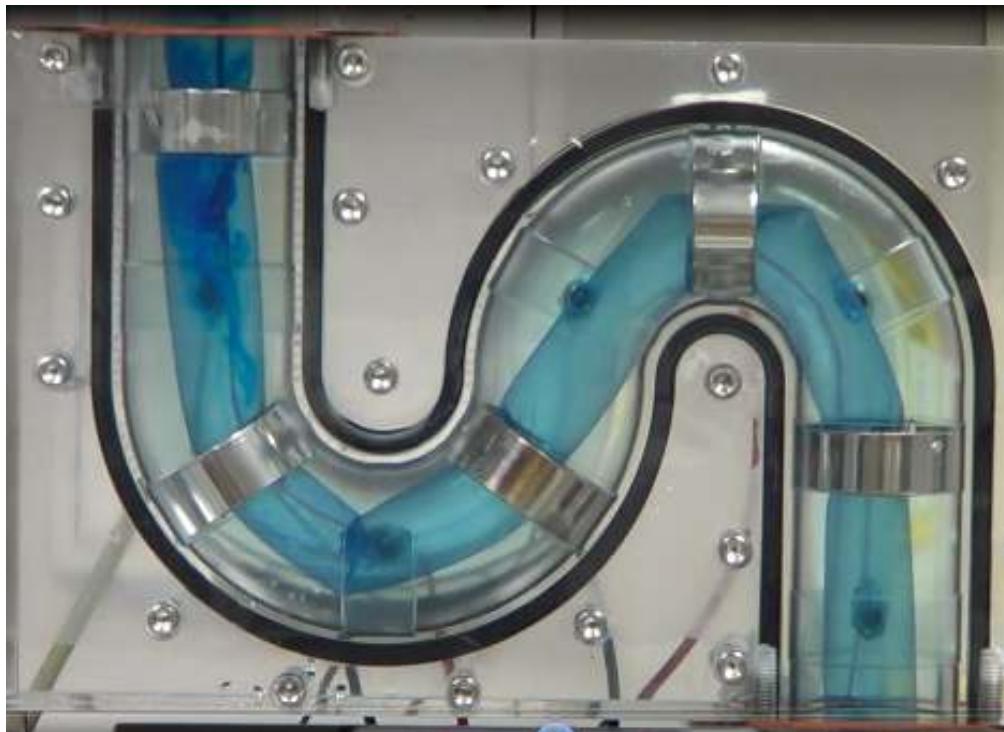


Figure 3.2: DIM set up for increased gap between contracting and relaxing rings.

Video of the model was recorded for the full 20 minute duration of each trial using a digital camcorder (HDR-CX220/B, Sony Electronics Inc., Tokyo, Japan). From the video footage, overall propagation time of solution through the model was determined by tracking how long it takes for methylene blue front to advance through the model. Specifically, three different sections of the model were looked at to determine how much gravity effects the overall propagation of digesta. The three sections looked at are illustrated in figure 3.3 below. Propagation tracking was done by following the methylene blue front through each segment. Time zero was taken as the point where the methylene blue begins entering the model. Time was tracked on the video.

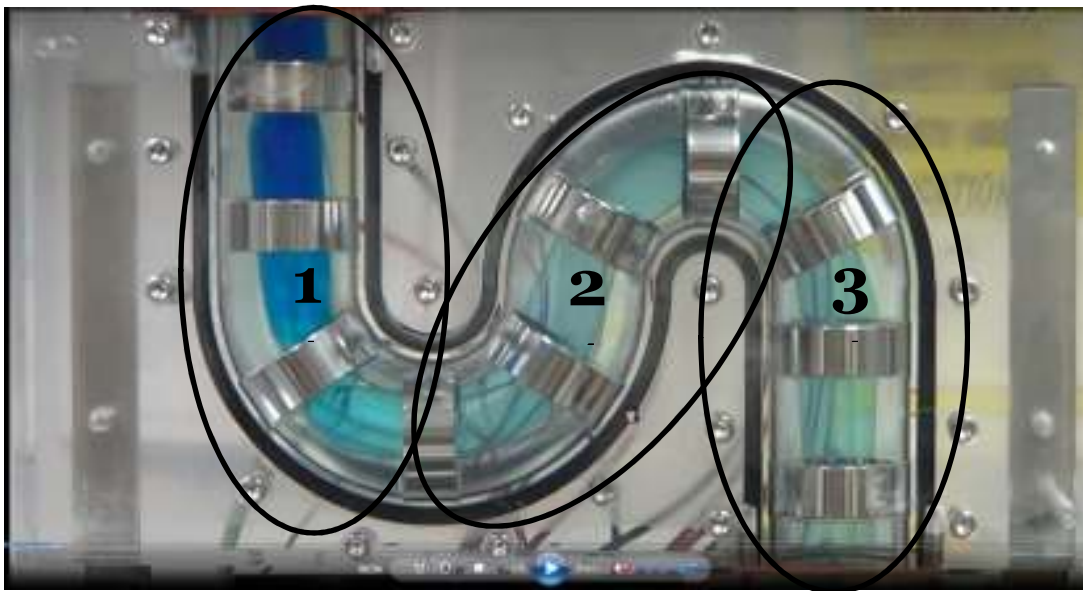


Figure 3.3: Sections of DIM looked at for determining overall propagation.

The key focus was using the estimated concentration of methylene blue solution in the membrane and concentration in recipient side to establish concentration gradient and from that estimate permeability of membrane. The concentration in the recipient fluid was determined using UV/Vis spectrophotometer (Evolution 300, Thermo Scientific Inc., Barrington, IL) while the concentration inside the membrane was estimated as geometric mean of expected concentration at beginning and end time

points depending on flow rate. For example, at a flow rate of 10mL/min into the membrane containing 300 mL of DI water, estimated concentration within membrane after 5min would be where 50 mL is derived from flow rate times time and 500ppm is the concentration of methylene blue in the solution perfused into the membrane.

The permeability of membrane was derived using techniques from study done by Fine and others (1995). Their study involved the perfusion of test solute in non-absorbable polyethylene glycol (PEG) into a 30cm segment of jejunum in live volunteers. They estimated permeability by taking the observed absorption rate J and dividing it by the observed concentration gradient ΔC . This gives a unit of permeability as $J/\Delta C$. These were used in the methylene blue trials along with a conversion factor of 0.6333. This was needed to convert units in DIM trials to units used in trial done by Fine and others (1995). Conversion factor was calculated from equation 1.

$$\frac{L}{57cm \cdot 20min} \times \frac{57cm \cdot 20min}{30cm \cdot 60min} \times \frac{60min}{h} = \frac{L}{57cm \cdot 20min} \times 0.6333 = \frac{L}{30cm \cdot h} \quad (\text{Eq.1})$$

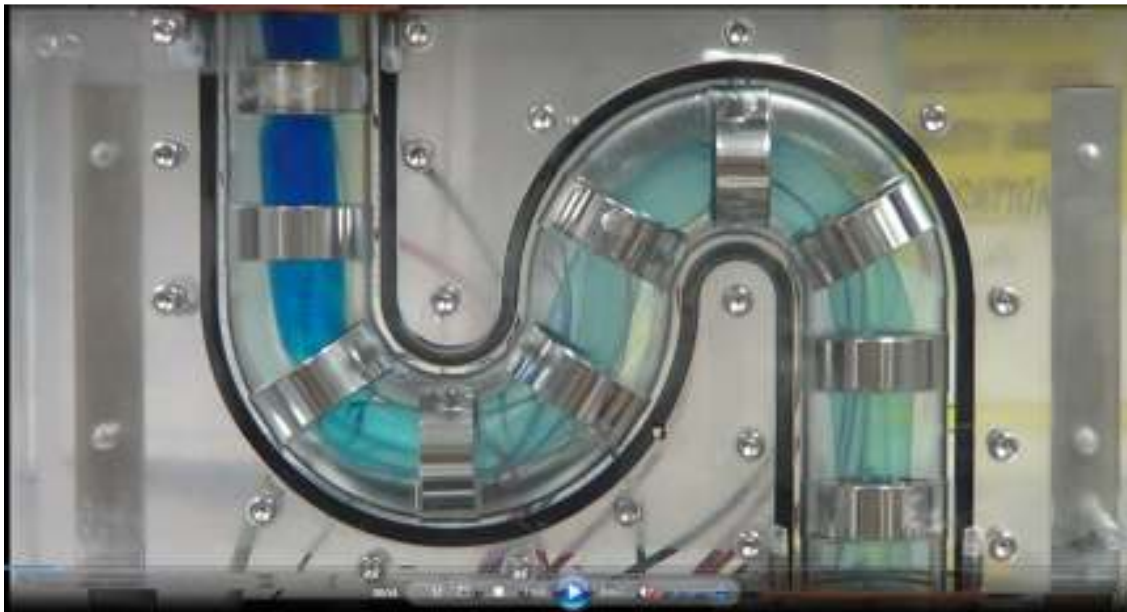


Figure 3.4: DIM during most of methylene blue trials. Methylene blue can be tracked easily through the model.

Results and Discussion

1. Flow rate

Permeability increased with flow rate but no significant difference ($p < 0.05$) between 10 and 15 mL/min flow rate (figure 3.5, table 3.1). It should be noted that in other studies such as Tharakan's studies indicates that flow rate does affect perceived permeability (Tharakan 2008); however the viscosity in their study was different than the methylene blue trials in DIM. As flow rate increases, permeability increases to a point, about 20 mL/min normally, and then stays constant. This is due to the faster flow rate negating the interface layer that can form between the fluid in the middle of the tube and the membrane edge due to predominant laminar flow found in the intestine (Fine and others 1995; Tharakan 2008).

As far as propagation goes, the second section of the model illustrated in figure 3.3 always took the longest time to go through, and there was no difference between the three test conditions except in the second section (Figure 3.6). This would indicate that gravity had an effect on digesta propagation. That was the reasoning for the sigmoid design of the DIM. Overall time for methylene blue front to pass through the DIM for standard conditions of 37°C, 0.001 Pa·s viscosity, and 10 mL/min flow rate was about 150s. Willmann and others (2003) studied intestinal transit time in rats using phenol red, and found that it takes roughly 2 h to get through all of the small intestine. Overall length of rat intestine is just 92 cm whereas length of membrane in DIM is 57 cm (Willmann and others 2003) and so doesn't make for an accurate comparison for transit time. In contrast, in the human intestine, it takes about 4 h for the digesta front to reach the end of the ileum and about another 4h for all the digesta to enter the cecum of the

large intestine depending on meal (Barrett and others 2010). Magnetic markers have been used to determine the transit time from mouth all the way through the duodenum. From these trials it was found that the transit time in the duodenum ranged from as little as 7 s to as much as 245 s (Weitschies and others 1999). Propagation time observed in the DIM fall within this range considering the length of the DIM for one pass is a little over twice as long as the human deodenum. This gives an estimated duodenal transit simulation in DIM of $150 \text{ s}/2=75 \text{ s}$. Most all of the other conditions tested also fell within this 7 s to 245 s range.

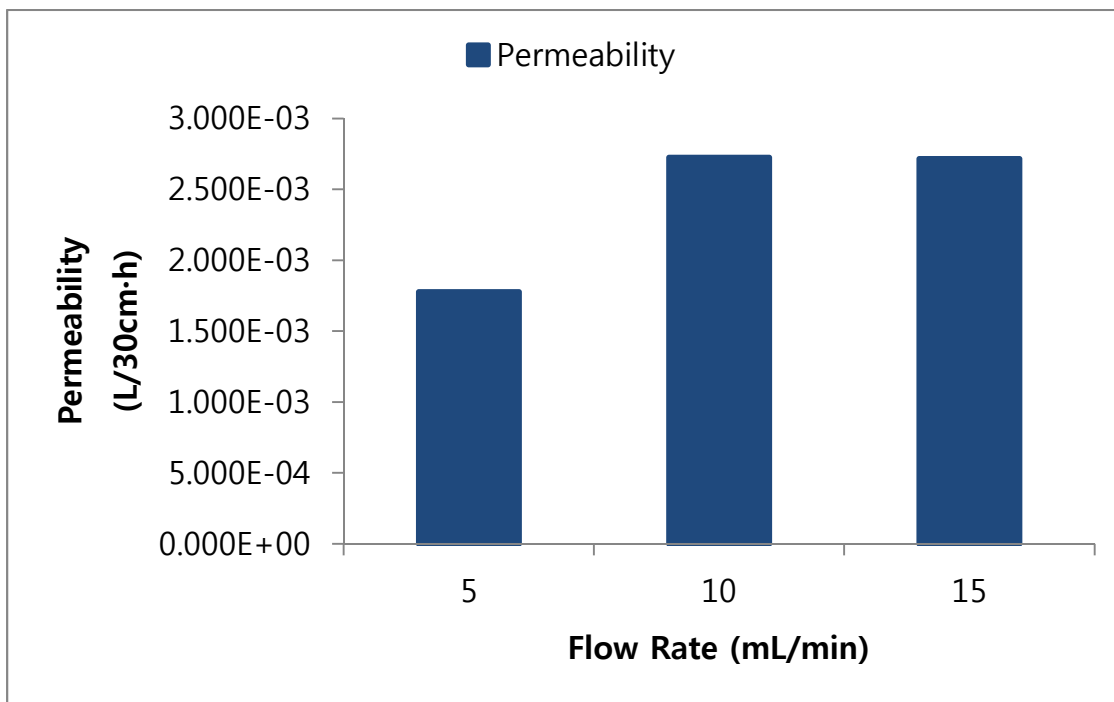


Figure 3.5: Permeability observed for given flow rates.

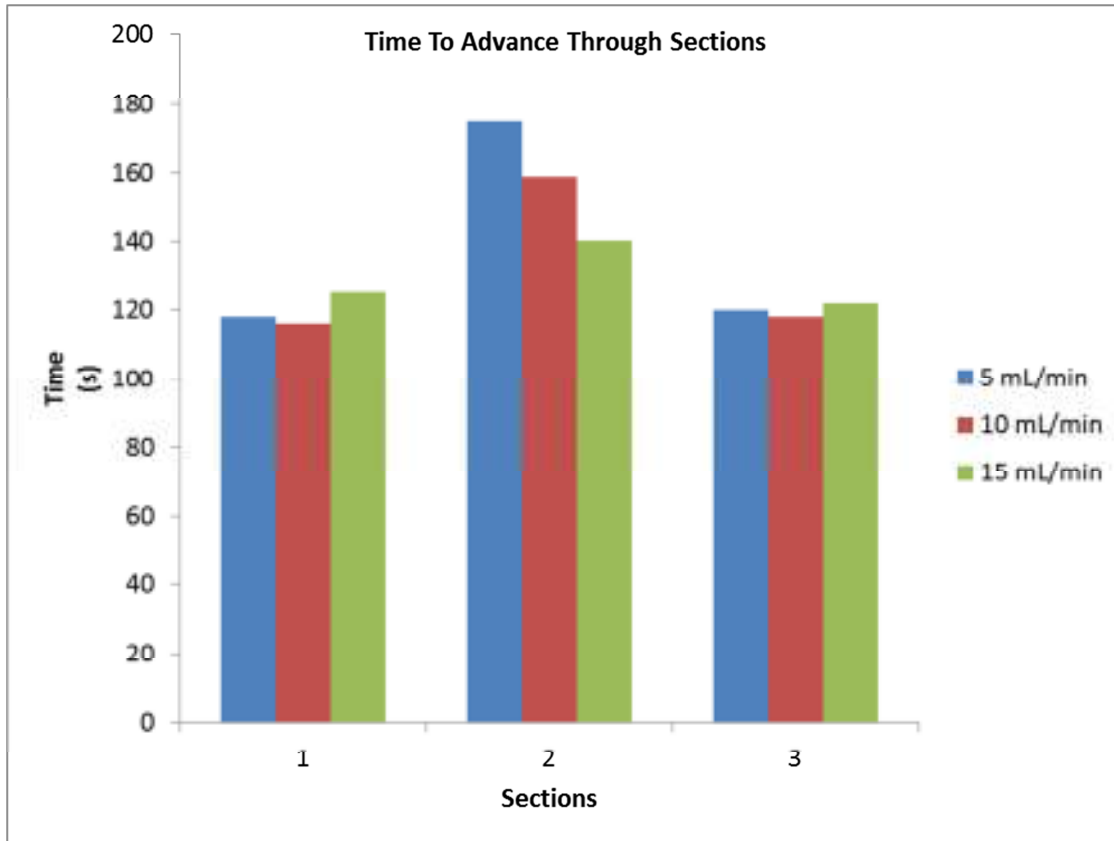


Figure 3.6: Time for methylene blue (MB) solution to advance through three different sections of model during flow rate trials.

Table 3.1: Permeability results from flow rate trial.

Flow Rate (mL/min)	Permeability (L/30cm·h)*
5	1.777E-3± 5.637E-5b
10	2.724E-3± 5.501E-6a
15	2.716E-3± 1.261E-05a

*Means with different letters are significantly different ($p < 0.05$) from each other.

2. Temperature

As seen in Table 3.2 and Figure 3.7 below, the permeability of methylene blue through the membrane is much greater in all three physiological temperature ranges as compared to room temperature. The value of permeability at normal body temperature in DIM was $4.420 \times 10^{-3} \text{ L/30cm}\cdot\text{h} \pm 1.615 \times 10^{-5}$ which was lower than found with *in vivo*

perfusion trials by Fine and others (1995). With urea as the solute tracked, they found a value of $4.000 \times 10^{-1} \pm 2.000 \times 10^{-2}$ L/30cm•h while for L-xylose they observed a value of $1.100 \times 10^{-1} \pm 1.000 \times 10^{-2}$ L/30cm•h. Both were observed with a flow rate of 10mL/min which was used in the DIM as well. This difference can be attributed to the fact that both urea and L-xylose are much smaller in molecular weight and diffuse more readily toward the membrane and through.

The propagation of methylene blue solution through the membrane increased as shown in Figure 3.10. Such results make sense when considering the Stoke-Einstein equation which is equation 1 below.

$$D_0 = \frac{k_B T}{6\pi\mu R_0} \quad (\text{Eq. 2})$$

This equation is commonly used to estimate diffusion coefficient for a solute through a solvent such as water. K_B in equation one is the Boltzmann's constant and doesn't change. The T in the equation represents temperature in K so an increase in temperature would increase this coefficient and as such a faster diffusion of methylene blue in all directions should be anticipated, especially in the direction of the flow.

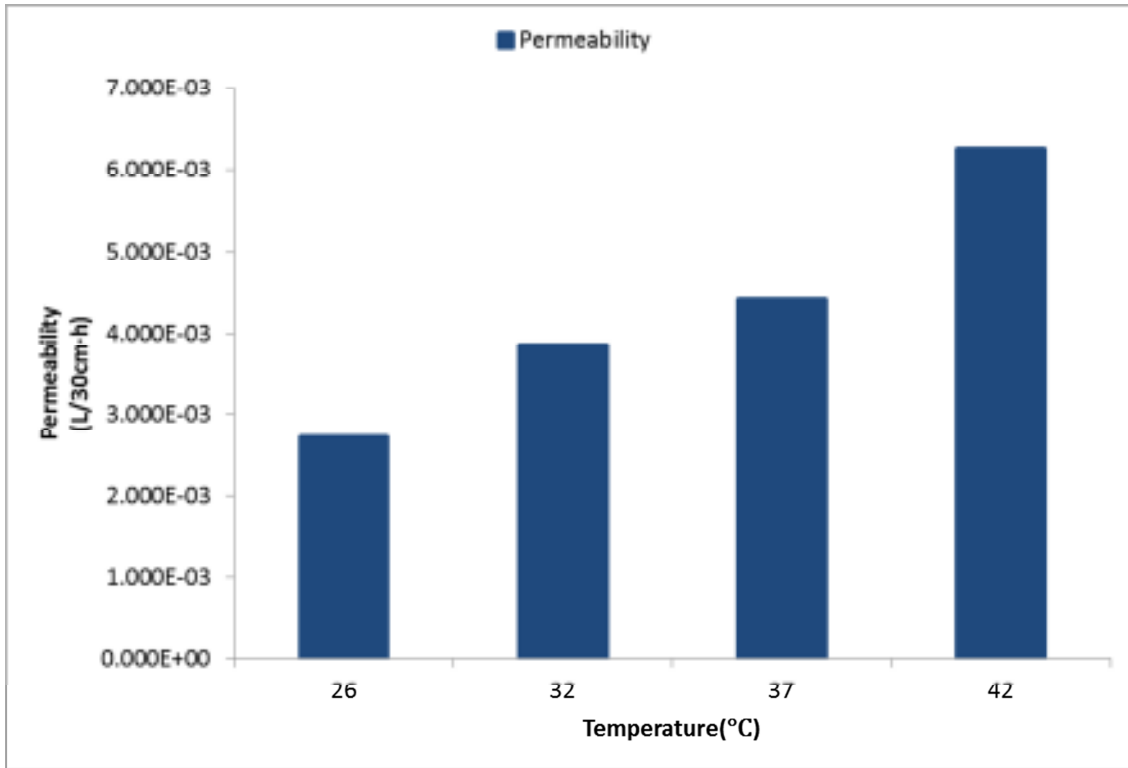


Figure 3.7: Permeability observed for given temperatures.

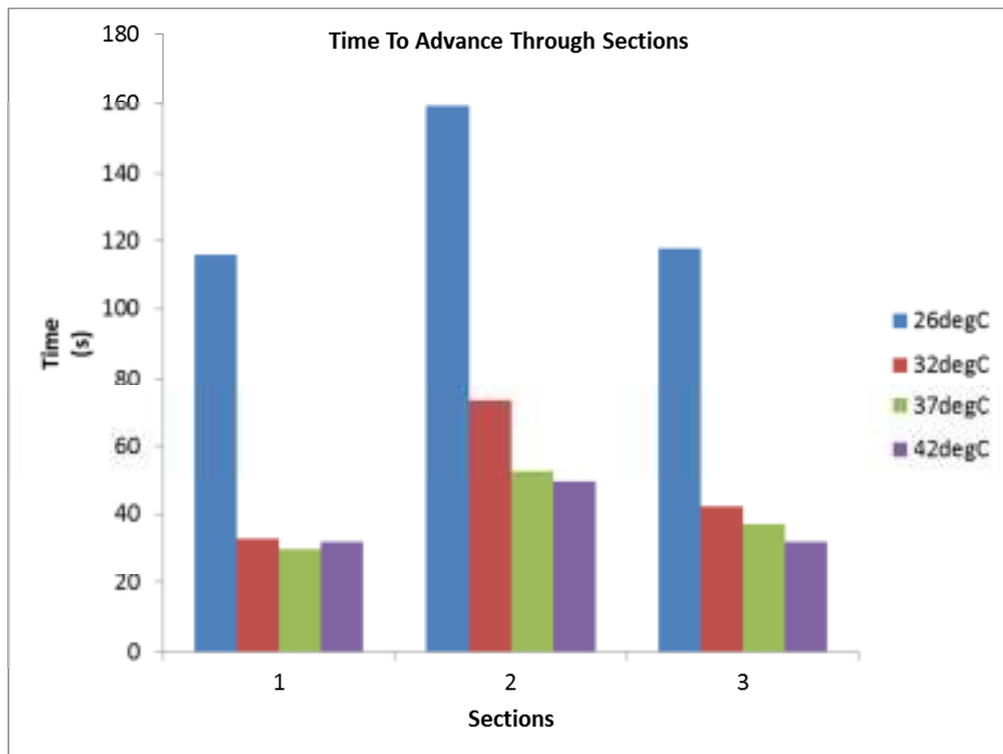


Figure 3.8: Time for MB solution to advance through three different sections during temperature trials.

Table 3.2: Permeability results from temperature trial.

Temperature (°C)	Permeability (L/30cm·h) *
26	2.724E-3± 5.501E-6d
32	3.854E-3± 2.848E-5c
37	4.420E-3± 1.615E-5b
42	6.259E-3± 2.773E-5a

*Means with different letters are significantly different ($p < 0.05$) from each other.

3. Viscosity

Figure 3.9 shows that with 6.01 Pa·s, a significant ($p < 0.05$) decrease in permeability of methylene blue. Table 3.3 shows the permeability values for the three viscosities, indicating the permeability decreased with the increase in the viscosity. The viscosity of digesta can vary greatly depending on solid content of the meal. These ranges found during *in vivo* trials ranged from 0.01 to 10 Pa·s (Ellis and others 1995). For this trial, three different concentrations of guar gum solutions to prefill the membrane 0.05, 0.1, and 0.2% were used. The temperature was kept at 37°C. The flow rate of 10mL/min and temperature of 37°C was used for remaining trials as well. From the Stokes-Einstein equation, it is expected that the perceived diffusion coefficient will decrease as the viscosity increases. Viscosity in Eq.1 is represented by μ . This decrease would not only slow down perceived forward propagation of methylene blue but also result in a smaller perceived permeability value of membrane. This is due to more resistance to solute moving toward and across membrane during test period. This greater resistance to solutes crossing the membrane was observed in both *in vivo* studies done by Ellis and others (1995) as well as Tharakan and others (2010) in regards

to glucose absorption. Tharakan and others (2010) reported that glucose absorption was greatly reduced with 0.5% guar gum, even with the action of segmentation.

Figure 3.12 indicated that as viscosity increases, the propagation rate decreases. Again as seen in Equation 3.1, an increase in viscosity means a decrease in diffusion coefficient throughout the medium in the membrane, in this case deionized water. As expected this means a decrease in the forward propagation of the methylene blue front. Viscosity values are kept fairly constant in the DIM whereas in actual intestinal tract, the viscosity varies with time in large part to the fact the jejunum absorbs bulk of water in the digesta. Our results indicate that the increasing viscosity may slow down propagation in the intestines.

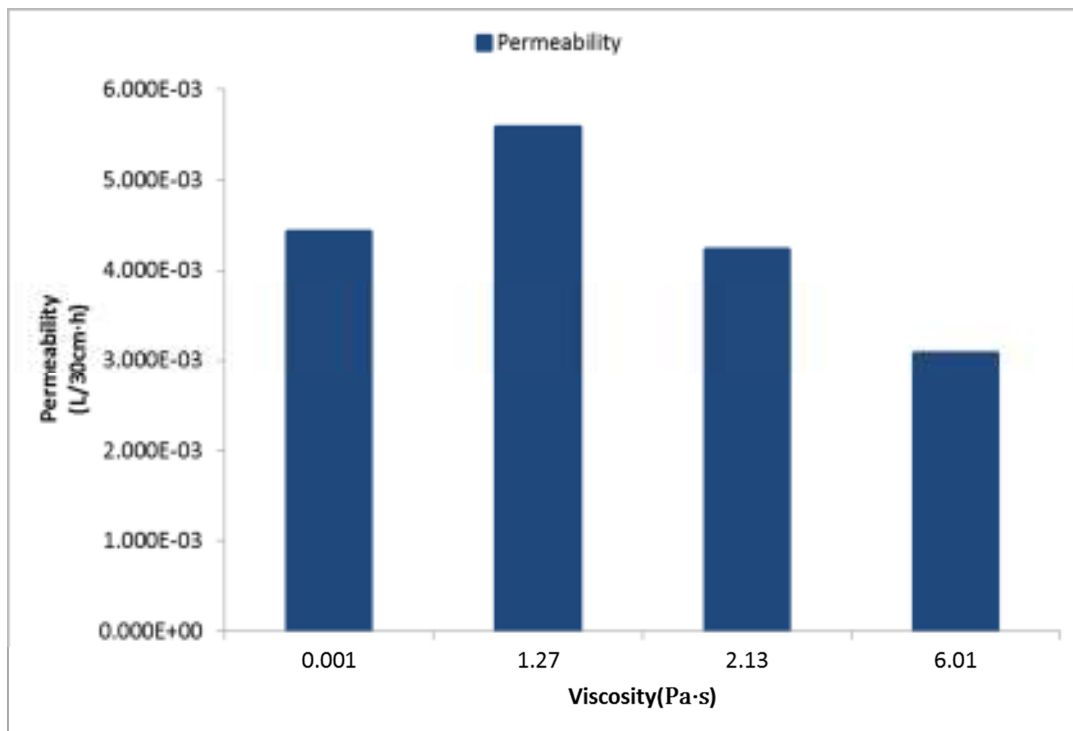


Figure 3.9: Permeability observed for given viscosities.

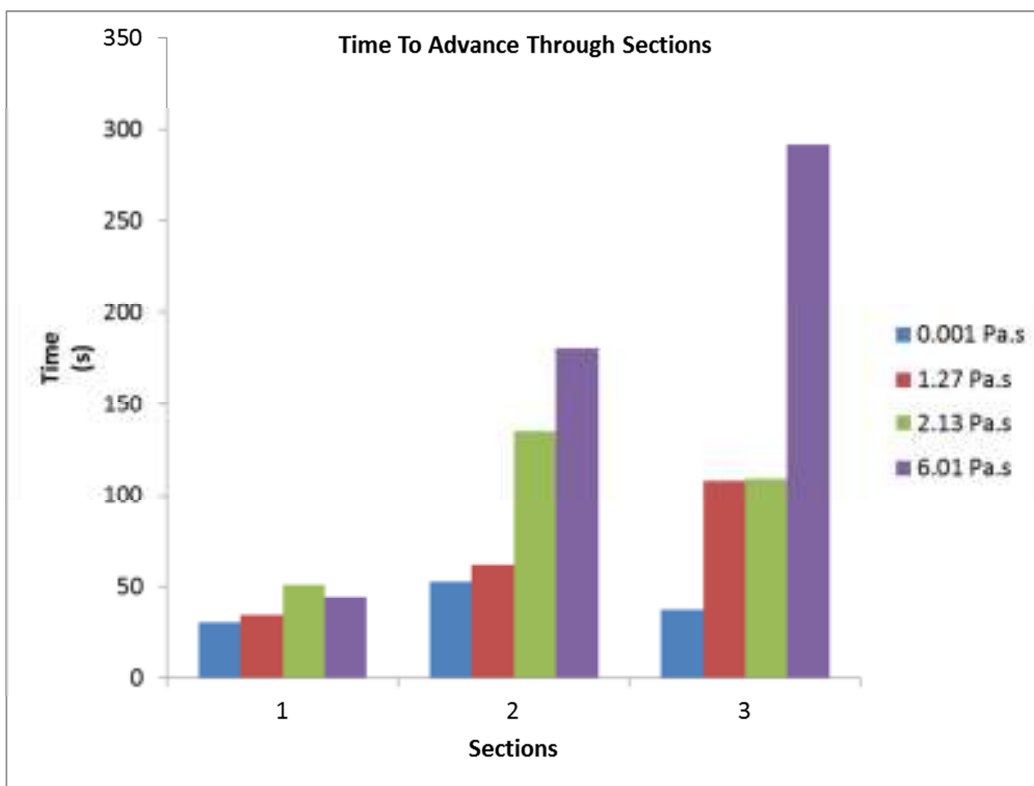


Figure 3.10: Time for MB solution to advance through three different sections during viscosity trials.

Table 3.3: Permeability results from viscosity trial.

Viscosity (Pa.s)	Permeability (L/30cm·h)*
0.001	4.420E-3± 1.615E-5b
1.27	5.574E-3± 1.415E-5a
2.13	4.229E-3± 5.970E-5c
6.01	3.078E-3± 1.868E-05d

*Means with different letters are significantly different ($p < 0.05$) from each other.

4 .Effect of segmentation

Results show that segmentation greatly improves perceived permeability value by about 4X, from $1.023 \times 10^{-3} \pm 5.688 \times 10^{-5}$ L/30cm·h without segmentation to $4.420 \times 10^{-3} \pm 1.615 \times 10^{-5}$ L/30cm·h value with segmentation. Figure 3.11 shows improved methylene blue absorption compared to no segmentation. As discussed earlier with flow rates, considering a s

straight laminar flow through the membrane sets up an interface layer between mobile fluid and the membrane boundary. It can be hypothesized that the mixing action brought on by the contractions could break up the interface layer and thus improve diffusion coefficient which would result in faster forward propagation. This would also lead to higher permeability as there would be less resistance for methylene blue to travel to and across the membrane. It was observed by Takahashi and others (2010) that only slight turbulent micromixing occurred during segmentation and overall the flow remained laminar. The Reynold's number for the test fluid in the DIM could be estimated as follows. With the test solution being an aqueous solution, ρ is the density of water, 1 kg/m^3 , and μ was taken as $0.001 \text{ Pa}\cdot\text{s}$, the viscosity of water at 20°C . The variable v is the flow rate of 10 mL/min or $1.667 \times 10^{-7} \text{ m}^3/\text{s}$ divided by cross-sectional area ($\pi \cdot 0.16 \text{ m}^2$) and then multiplied by diameter 0.32 m . This yields Re number of 6.633×10^{-4} which is much less than 2100 indicating flow to be laminar (Takahashi 2011; Tharakan 2008). Increased permeability in that case was thought to be due to the close physical proximity of nutrients to the intestinal wall during segmentation contraction. It should be noted that their observations were made from ileum of pig small intestine as well as cecum and colon. The digesta by this point is very viscous having lost most of its water content. Also noted is the fact that a few vortices were noted during recording of propagation of methylene blue front indicating a bit of turbulent micromixing occurring immediately after a segmentation contraction (Figure 3.12). Figure 3.13 shows the propagation rate for each section comparing with/without segmentation. It shows with segmentation, the propagation rate significantly increased. The forward propagation results appear at a glance to be on the contrary to what has been reported in the literature. Barrett and others (2010) stated that segmentation contractions served the purpose of not only mixing but of slowing down the overall forward

propagation of digesta. This is far from what was shown in the DIM. It was encouraging to see that the permeability results for segmentation were much closer to the numbers calculated by Fine and others (1995) who reported $4.000 \times 10^{-1} \text{ L/30cm}\cdot\text{h}$ for urea and $1.100 \times 10^{-1} \text{ L/30cm}\cdot\text{h}$ for L-Xylose. These numbers again show a much larger permeability due to the much smaller size of those solute molecules compared to methylene blue. However when looking at mannitol in the Fine study, values observed were $3.000 \times 10^{-2} \text{ L/30cm}\cdot\text{h}$ which is closer to the value found for segmentation trial in DIM of $4.420 \times 10^{-3} \text{ L/30cm}\cdot\text{h}$. Mannitol is smaller than methylene blue at about 182 g/mol but this is closer to the 319 g/mol of methylene blue.

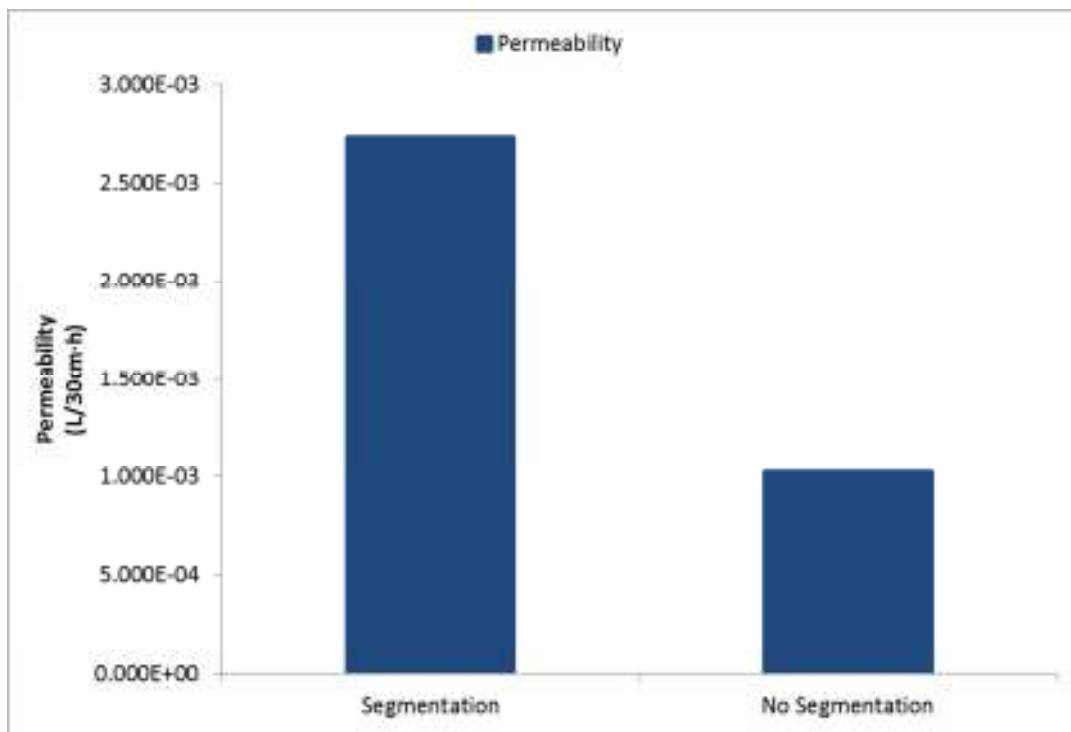


Figure 3.11: Permeability observed given presence or absence of segmentation.



Figure 3.12: Close up of DIM right after a contraction. Note two faint vortices formed right after the contraction, which went away less than a second after contraction.

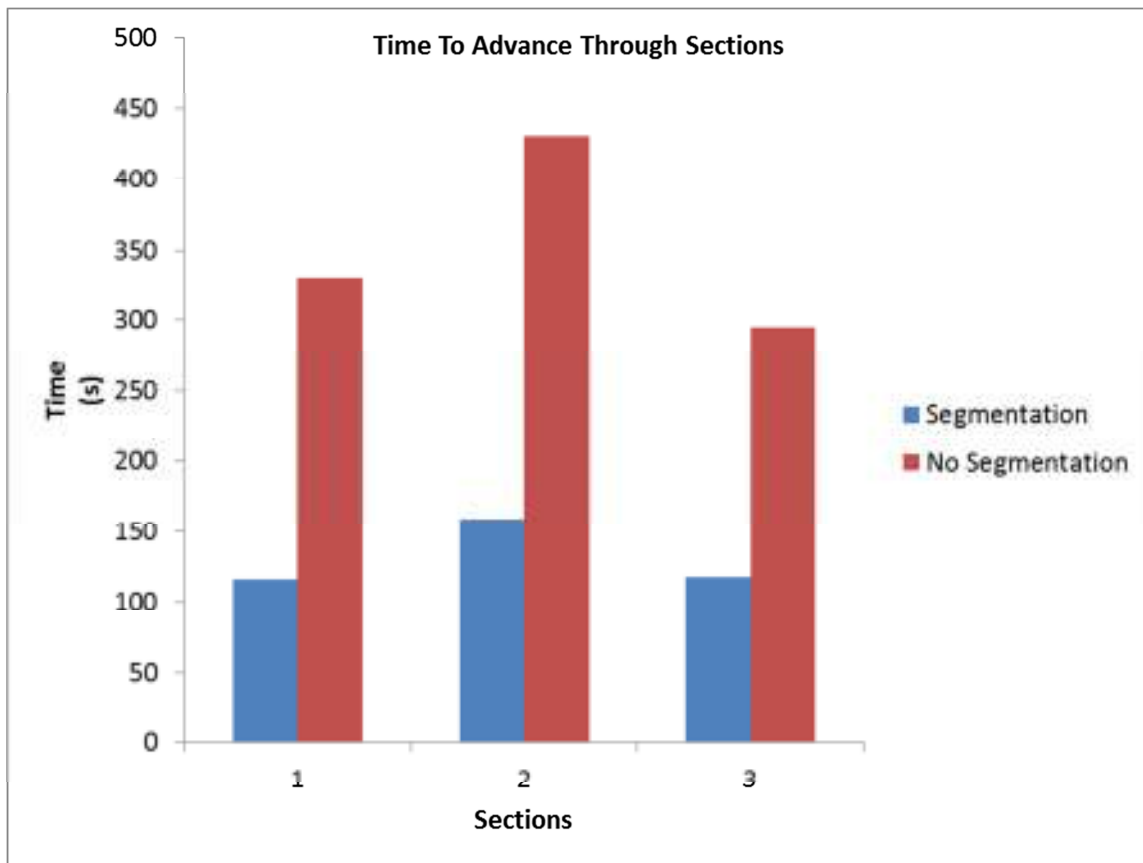


Figure 3.13: Time for MB solution to advance through three different sections during segmentation trials.

5. Model Orientation

Figure 3.14 shows significant increase in permeability to methylene blue into the recipient fluid with the more vertical orientation. There was a significant difference in permeability values observed between more horizontal orientation and more vertical orientation. The value for original horizontal placement was $4.420 \times 10^{-3} \pm 1.615 \times 10^{-5}$ L/30cm·h which was less than the more vertical arrangement of $6.527 \times 10^{-3} \pm 5.688 \times 10^{-5}$ L/30cm·h. The concern about always operating the DIM in that arrangement however is that retention of larger food particles for more complete digestion may not occur as much as the original placement would be better able to collect larger particles in the lowest point of the sigmoid where section 1 and section 2 meet.

The most interesting results encountered thus far are the propagation data illustrated below in Figure 3.15. It was expected that the more vertical orientation of the DIM would result in a faster propagation time but what was actually observed was a slightly slower propagation of the methylene blue. The reason behind this most likely lies in the sigmoid shape as well. Though in this arrangement, the model appears more vertical than horizontal, if one looks at the sigmoid path itself it can be seen that there are actually more instances of horizontal flow. Upon entering the DIM, the solution has to travel forward toward where section 1 meets section 2. There's a slight vertical drop at this point but then it's another horizontal trek in the opposite direction than in section 1 and then drops again before moving horizontally toward the exit. So for most of the time spent by the digesta in the DIM in this orientation would actually be horizontal flow thus slowing it down.

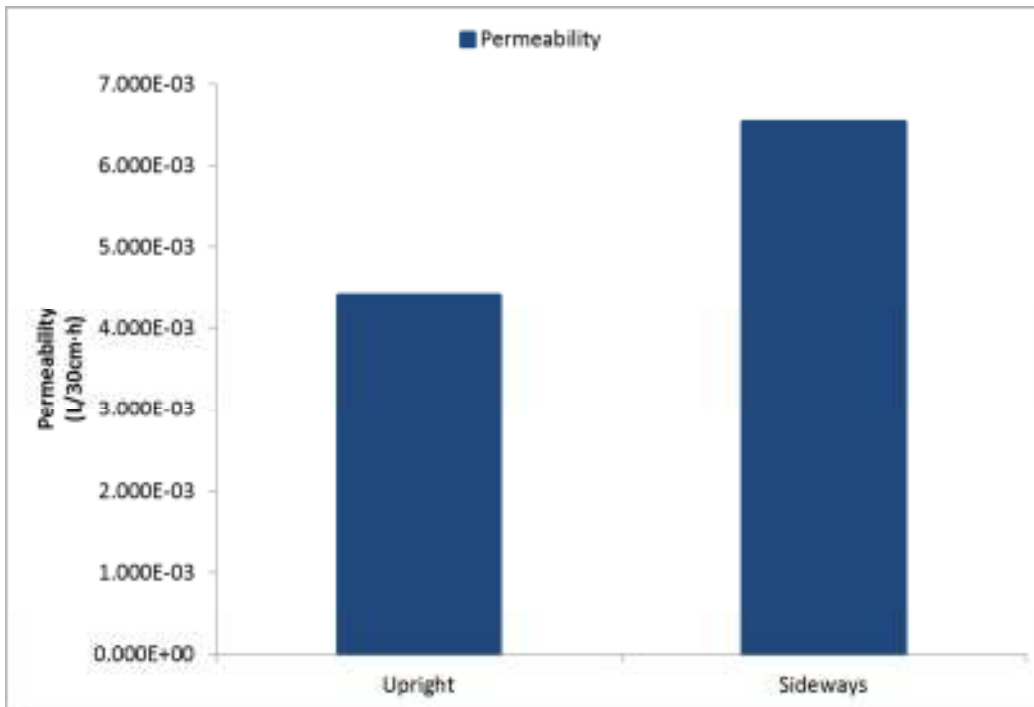


Figure 3.14: Permeability observed given particular orientation

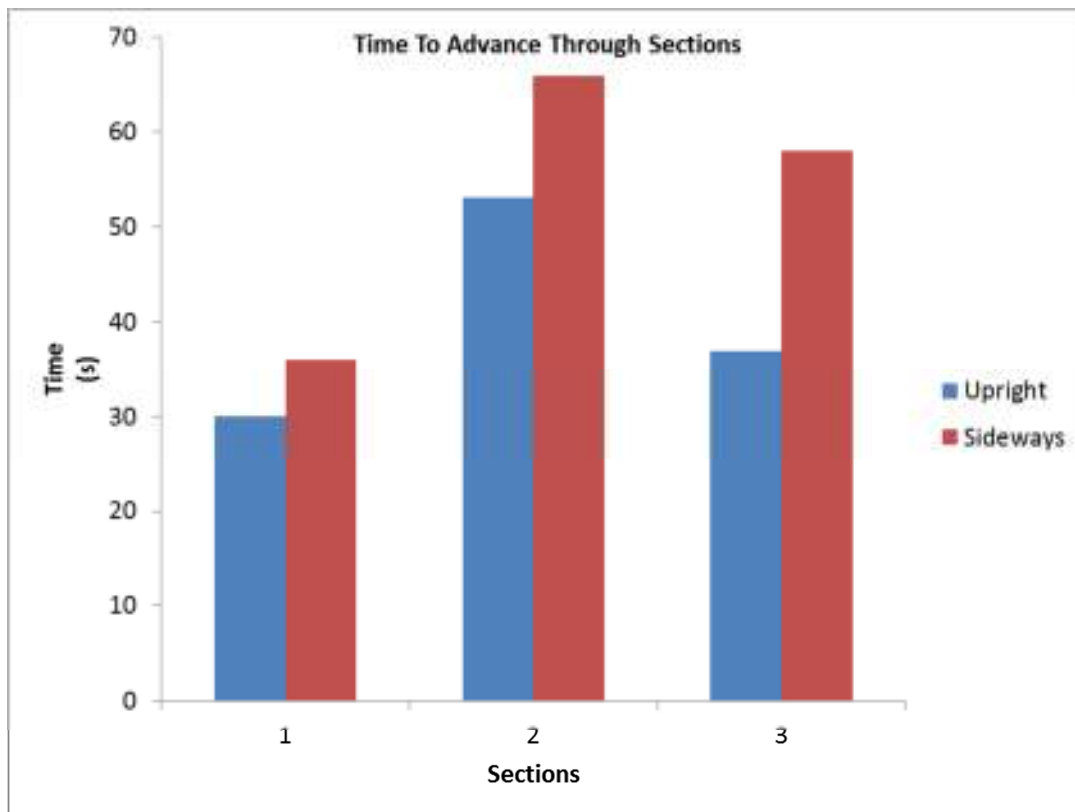


Figure 3.15: Time for MB solution to advance through three different sections during orientation trials.

6. Segmentation Placement Effects

Figure 3.16 shows greater permeability of methylene blue with all rings in place. Table 3.4 shows the results of different placement of segmentation. The permeability values for both altered placement of segmentation rings were significantly less than the original, regularly spaced condition. The third condition tested where distance between contracting and relaxing rings was doubled was the lowest, almost $\frac{1}{4}$ that of the original set up, at $1.974 \times 10^{-3} \text{ L}/30\text{cm}\cdot\text{h}$. As far as placement of segmentation contractions, it appears important that pairs of alternating contractions must be in close proximity of each other, about 4cm, in order to get good mixing and turbulent flow to increase both perceived permeability and propagation. Segmentation contractions *in vivo* can be irregularly or regular but widely spaced (Barrett and others 2010; Tharakan 2008). With that in mind, test were done on two different segmentation patterns were used and their effects on permeability and propagation tested.

The value of permeability from original set up are higher and thus closer to the *in vivo* values found in trial done by Fine and others (1995). This suggests the contractions are for the most part regularly spaced during digestion in the human intestine. The observed propagation was much slower in the trial with 13cm separation between contracting and expanding rings and 7 cm distance between contraction and expansion rings (Figure 3.19). This was expected as the great distance reduces the turbulent mixing that helps to facilitate the forward diffusion of methylene blue through the deionized water in the membrane.

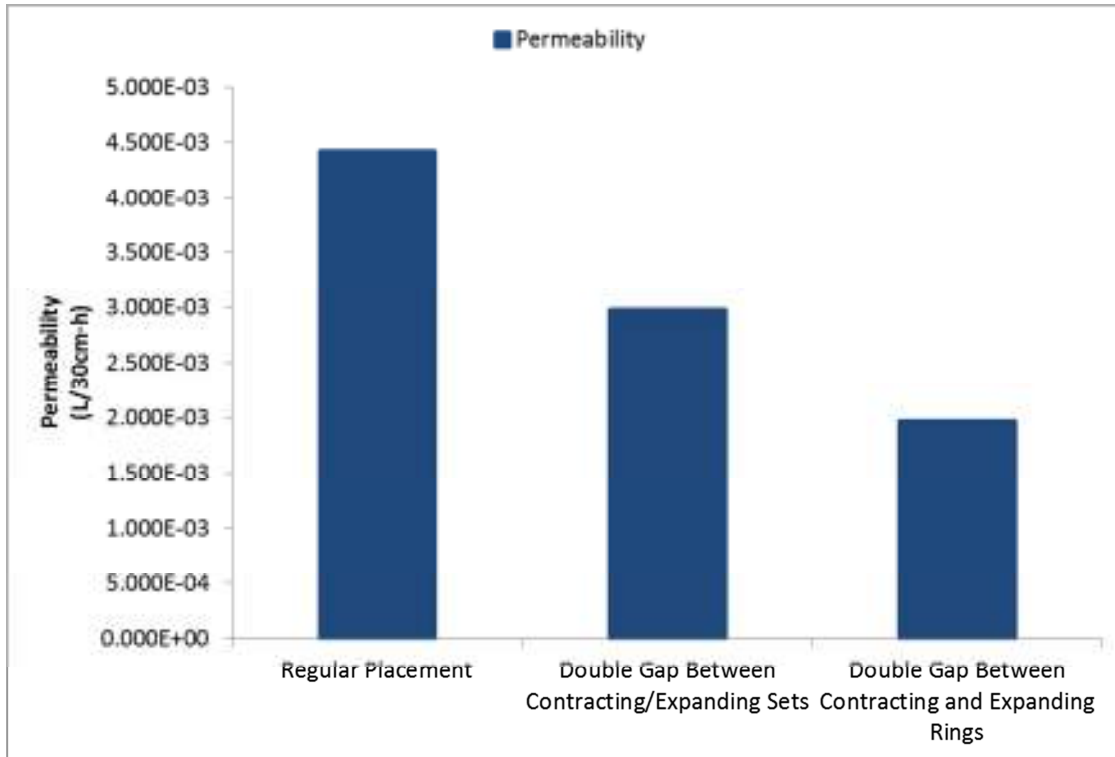


Figure 3.16: Permeability observed for given segmentation placement

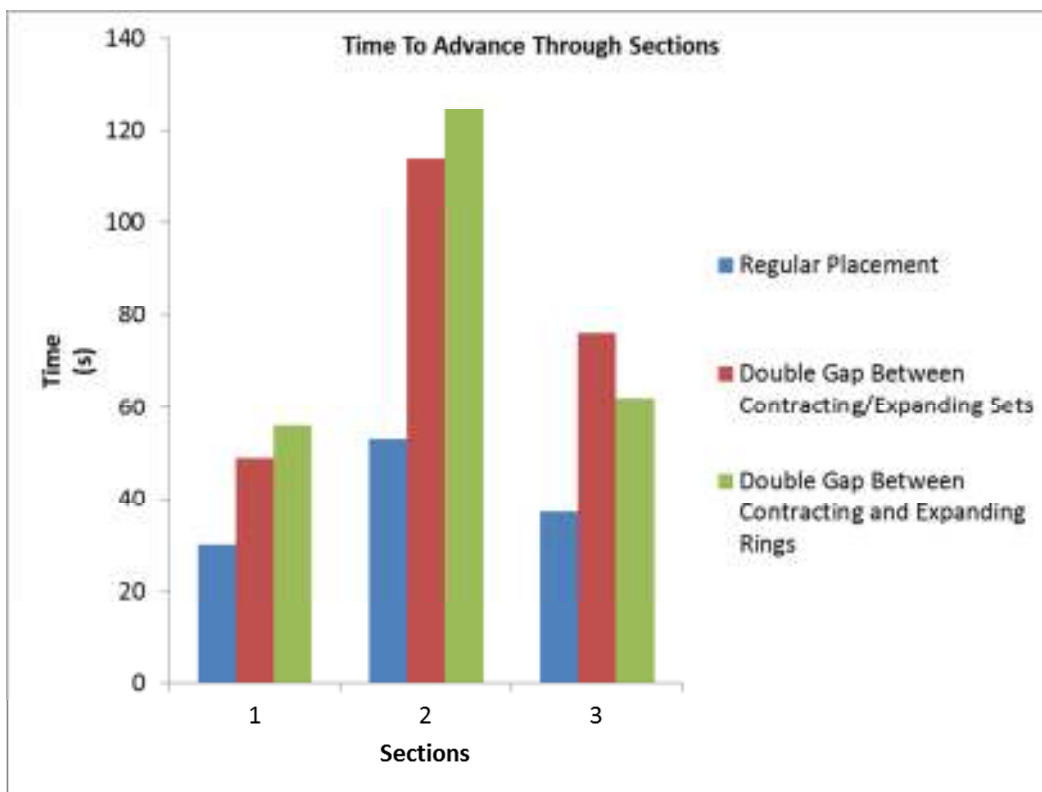


Figure 3.17: Time for MB solution to advance through three different sections during segmentation placement trials.

Table 3.4: Permeability results from segmentation placement trial.

Segmentation Configuration	Permeability (L/30cm·h)*
Regular Placement	4.420E-3± 1.615E-5a
Double Gap Between Contracting/Expanding Sets	2.973E-3± 2.689E-5b
Double Gap Between Contracting and Expanding Rings	1.974E-3± 4.618E-05c

*Means with different letters are significantly different ($p < 0.05$) from each other.

7. Methylene blue summary discussion

Methylene blue was suitable for study in the effect of various physiological conditions in intestinal permeability and propagation of digesta through DIM. For the most part it was a fair marker for determining permeability values for the membrane, and the results show a good agreement with those derived in the *in vivo* perfusion study done by Fine and others (1995). Methylene blue has high molecular weight of 319 g/mol compared to the test solutes urea, L-xylose, and mannitol used in their study. However, it is clear that as molecular weight of solute increases, permeability decreases as seen in the values, arranged from greatest perceived permeability to least with molecular weights in parenthesis, urea (60.06 g/mol), L-xylose (150.13 g/mol), and mannitol (182.17 g/mol). Figure 2.18 below summarizes the data from the DIM and *in vivo* perfusion study done by Fine and others (1995) under conditions of 0.001 Pa·s viscosity, 37°C, and flow rate of 10 mL/min.

Even during the trial without the segmentation contraction, the forward propagation observed didn't even reach 30 min while according to the phenol red trials done on rat intestine by Willmann and others (2003), transit of the entire 96 cm rat intestine took a little over 1 h. However when compared to duodenal transit times studied by Weitschies and others (1999), the DIM transit times fall within their range.

Again it needs to be noted that *in vivo* there is no fluid except what is secreted when needed. For the DIM, the membrane needs to be prefilled with water or a buffer solution depending on recipient fluid used. This fluid filled state results in diffusion of methylene blue forward with the flow as well as toward the membrane walls. This added forward motion of methylene blue front to the flow rate results in faster perceived propagation, especially during conditions of very low viscosity and high temperatures. It should be noted here that slight solvent drag did occur with these trials but not a significant level. This shows the potential for the DIM to actively remove water from digesta like what is done in actual small intestine.

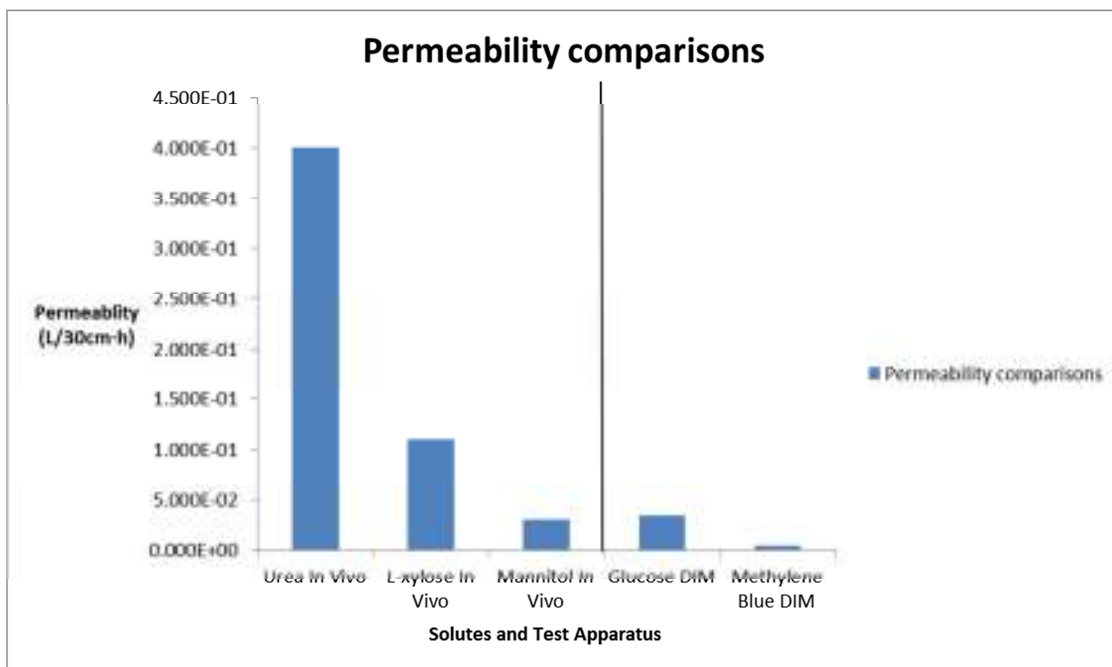


Figure 3.18: Comparison of permeability values from both *in vivo* trials by Fine and others (1995) and DIM trials. The solid line divides the *in vivo* results on left from DIM results on right. Glucose results from earlier permeability trial done with DIM.

Conclusions

By utilizing methylene blue solution, permeability for the membrane used in the DIM was calculated. Propagation rates of intestinal contents were studied. These values were then compared to *in vivo* data available in literature. The kinetics information about propagation and absorption was obtained with the help of the DIM, which is useful for understanding the food digestion process. Good correlation was observed between factors such as temperature, viscosity, segmentation, and orientation on absorption of nutrients and on digesta propagation. The results of these trials were backed up by *in vivo* data and thus by utilizing the proper parameters, the DIM can accurately simulate digestion in the human small intestine.

References

- Barrett KE, Brooks HL, Boitano S, Barman SM. 2010. Section V Gastrointestinal Physiology. Ganong's Review of Medical Physiology 23rd Edition ed: McGraw Hill Medical. p. 429-87.
- Ellis P, Roberts F, Low A, Morgan L. 1995. The effect of high-molecular-weight guar gum on net apparent glucose-absorption and net apparent insulin and gastric-inhibitory polypeptide production in the growing pig - relationship to rheological changes in jejunal digesta. *British Journal of Nutrition* 74(4):539-56.
- Fine K, Santanna C, Porter J, Fordtran J. 1995. Effect of changing intestinal flow-rate on a measurement of intestinal permeability. *Gastroenterology* 108(4):983-9.
- Fordtran JS, Rector FC, Jr., Ewton MF, Soter N, Kinney J. 1965. Permeability characteristics of the human small intestine. *The Journal of Clinical Investigation* 44(12):1935-44.
- Larhed A, Artursson P, Grasjo J, Bjork E. 1997. Diffusion of drugs in native and purified gastrointestinal mucus. *Journal of Pharmaceutical Sciences* 86(6):660-5.
- Linnankoski J, Makela J, Palmgren J, Mauriala T, Vedin C, Ungell AL, Lazorova L, Artursson P, Urtti A, Yliperttula M. 2010. Paracellular Porosity and Pore Size of the Human Intestinal Epithelium in Tissue and Cell Culture Models. *Journal of Pharmaceutical Sciences* 99(4):2166-75.
- Sherwood L. 2011. *Fundamentals of Human Physiology*: Cengage Learning.
- Sonavane G, Tomoda K, Sano A, Ohshima H, Terada H, Makino K. 2008. *In vitro* permeation of gold nanoparticles through rat skin and rat intestine: Effect of particle size. *Colloids and Surfaces B-Biointerfaces* 65(1):1-10.
- Takahashi T. 2011. Flow Behavior of Digesta and the Absorption of Nutrients in the Gastrointestine. *Journal of Nutritional Science and Vitaminology* 57(4):265-73.
- Tharakan A. 2008. Modeling of physical and chemical processes in the small intestine. [Doctor of Engineering]. Birmingham, UK: The University of Birmingham. 286 p.

Tharakan A, Norton IT, Fryer PJ, Bakalis S. 2010. Mass Transfer and Nutrient Absorption in a Simulated Model of Small Intestine. *Journal of Food Science* 75(6):E339-E46.

Weitschies W, Cardini D, Karaus M, Trahms L, Semmler W. 1999. Magnetic marker monitoring of esophageal, gastric and duodenal transit of non-disintegrating capsules. *Pharmazie* 54(6):426-30.

Willmann S, Schmitt W, Keldenich J, Dressman J. 2003. A Physiologic model for simulating gastrointestinal flow and drug absorption in rats. *Pharmaceutical Research* 20(11):1766-71.

CHAPTER 4

**COMPARISON OF SHAKING WATER BATH AND DYNAMIC INTESTINAL
MODEL (DIM) IN SIMULATING STARCH DIGESTION AS AFFECTED BY
GASTRIC DIGESTION AND BILE**

¹ Wright, N.D. and Fanbin Kong. To be submitted to *Food Engineering*.

Abstract

In vitro digestion trials are frequently used to study digestion of starchy foods. Because intestine is the major site for starch digestion, trials often omit gastric phase. During simulated intestine phase, enzymes including glucosidase were used, but bile juice was often omitted although it is critical for human digestion. However, gastric digestion as well as bile is components that significantly affect digestion of starchy foods in intestine. The objective of this study was to investigate influence of gastric and pre-gastric phase of digestion and bile salts on bread digestion, focusing on starch breakdown to glucose in simulated intestinal environment using both shaking water bath and DIM. For these trials, 8 different samples were looked at representing 4 different digestive conditions with 2 different digestion simulation techniques: shaking water bath and DIM. Four conditions tested were duodenal and salivary enzymes only, first condition with gastric enzymes added, first condition with bile salts added, and finally one with all enzymes present. Results indicate bile salt significantly affected rate of bread digestion in intestine. Samples that underwent digestion in the present of gastric enzymes and bile showed the highest level of available glucose. DIM produced the highest glucose levels in all four conditions compared with sample run in shaking water bath. This shows the greater efficiency of digestion that occurs in the DIM.

Introduction

Previous studies with the DIM dealt primarily with the permeability of the membrane used and thus how well it would represent the human small intestine when it comes to absorbing nutrients. Before these nutrients can be absorbed though, they must be broken down during the process of digestion. Food must be broken down into smaller macromolecules such as glucose in order to be converted to the energy needed for

everyday life processes. Various different enzymes are utilized throughout the entire digestive system for this purpose. Examples of these enzymes include pepsidases such as trypsin for protein breakdown and amylases responsible for breakdown of starch into glucose(Barrett and others 2010). The effectiveness of the enzymes can be altered by inhibitors which work either on the enzyme itself or the substrate.

Depending on the situation, digestive enzyme inhibition can be beneficial or detrimental. Such detrimental effects from enzyme inhibition can be seen from protein digestion inhibition in foods such as legumes. It becomes necessary to heat such foods to temperatures high enough to ensure these inhibitors are denatured (Zahnley 1984).

There are also beneficial effects from inhibiting digestion enzymes, particularly amylases. By inhibiting amylases, one would be inhibiting the breakdown of starch into glucose. This would be a major advantage to those suffering from diabetes and have a constant need to keep blood glucose levels under control. The specific mechanism for glucose uptake suppression is not always well understood. One study looking at pine needle extract for example determined that use of such an extract greatly reduced glucose uptake and may exhibit α -glucosidase inhibitory characteristics but how exactly is not fully understood (Kim and others 2005). Other studies have found that the inhibition comes about by binding of the inhibitor with the substrate, preventing the enzyme to attach with the substrate and perform its function. This was determined to be the case with aliphatic compounds, namely fatty acids as well as polyphenols including epicatechin-methylgallate and rutin (Takahama and Hirota 2010). Further studies have shown that bile salts used in the digestive system to help emulsify fats may also bind with starch or more specifically the helical structure of amylose to bring about inhibition (Takahama and Hirota 2011).

The purpose of this study was to investigate the inhibitory action of bile salts using both shaking water bath and DIM digestion. Results from both trials were compared to each other as well as with *in vivo* and *in vitro* results from literature. Also looked at was how the availability of glucose from food matrix was affected by the inclusion of a gastric step. This is a step often left out in digestion as the focus of most *in vitro* glucose availability trials are on amylases found in saliva and in pancreatin. It can be hypothesized though that the breakdown of proteins by gastric enzymes may result in a greater ease of starch digestion with amylases.

Materials and Methods

Materials

The bread used for the trials was Nature's Own™ whole wheat bread. A Ninja mini food processor was utilized for the mechanical breakdown of bread samples. All enzymes and other digestive aids for the digestion studies, including amylase, pepsin, mucin, pancreatin, and bile salts, were provided by Sigma-Aldrich. They also supplied the dinitrosalicylic acid and Rochelle salt for the formulation of DNS solution to measure glucose levels spectrophotometrically. Most of the various salts such as Magnesium Chloride and Sodium Chloride for making simulated digestive juices were supplied by Fisher Scientific or Sigma Aldrich. The exception to this being Urea which was supplied by Bio-Rad.

Methods

1. Simulated digestive juice preparation

All salt solutions for the four simulated digestive juices were prepared as outlined in Figure 4.1 below slightly modified from formulation used by Hur and others (2009) as much a week or so in advance of actual trials. On the day of the trials, the enzymes

were added to their respective solutions: salivary, gastric, duodenal, and bile. Amounts of enzymes used were scaled to the volume utilized in the trials which were 10mL for salivary juice and bile juice as well as 20mL of gastric and duodenal juice based on recommendations for *in vitro* digestion trials stated in Versantvoort and others (2004). All juices were then adjusted to their proper pH shown in Figure 4.1.

Saliva Stock Solution	Gastric Stock Solution	Duodenal Stock Solution	Bile Stock Solution
500 mL DI water	500 mL DI Water	500 mL DI Water	500 mL DI Water
0.0585 g NaCl	2.752 g NaCl	7.012 g NaCl	5.29 g NaCl
0.0745 g KCl	0.824 g KCl	0.564 g KCl	0.376 g KCl
1.05 g NaHCO ₃	0.266 g NaH ₂ PO ₄	3.388 g NaHCO ₃	5.785 g NaHCO ₃
	0.399 g CaCl ₂ •2H ₂ O	0.08 g KH ₂ PO ₄	
	0.306 g NH ₄ Cl	0.05 g MgCl ₂	
0.2 g urea	0.085 g urea	0.1 g urea	0.25 g urea
	6.5 mL HCl	180 µL HCl	150 µL HCl
Simulated Saliva	Simulated Gastric Juice	Simulated Duodenal Juice	Simulated Bile Juice
Amount: 100 mL stock	Amount: 100 mL stock	Amount: 100 mL stock	Amount: 100 mL stock
0.1 g mucin	0.5 g pepsin	1.8 g pancreatin	6 g bile
0.2 g α-amylase	0.6 g mucin	0.3 g lipase	
pH: 6.8 +/- 0.2	pH: 1.30 +/- 0.02	pH: 8.1 +/- 0.2	pH: 8.2 +/- 0.2

Figure 4.1: Components of digestive juices used.

2. Pre-intestinal phase

For each condition tested, 20g of bread was used. Bread was weighed to 104g and minced finely in Ninja food processor. Ground samples were then weighed into four equal portions of 20g in four separate 400mL beakers. 10mL of simulated salivary juice was added to each sample and a glass rod was used to gently incorporate bread with salivary juice for 2min to represent chewing. 20mL of simulated gastric juice was then added, following the method of Hur and others (2009). For the conditions not involving gastric digestion, an equal volume of gastric juice without the gastric enzymes was used

instead. Samples were then placed in a shaking water bath (290400, Boekel Scientific Inc., Feasterville, PA) set to 37°C and speed setting of 120rpm. Samples were agitated in the water bath for 60min. Beakers were covered with parafilm to prevent condensation from dripping into the beakers from the lid above.



Figure 4.2: Diagram of the pre-intestinal phase of digestion trials. Top left shows bread sample minced in mini food processor. Top right show incorporation of salivary juice with one sample. Bottom shows beakers in the shaking water bath after receiving gastric juices.

3. Intestinal phase: shaking water bath

For the four samples that underwent digestion in the shaking water bath, orbital shaking was ceased and 20mL of simulated duodenal juice along with 10mL of simulated bile juice. For the sample going through digestion without bile, 10mL of bile juice without the bile was added instead. Orbital shaking of the same speed setting of 120rpm was resumed and digestion was carried out for 2h.

1mL aliquots of digesta samples were collected at the following times: 0min (right before intestinal juices were added), 3min, 6min, 10min, 20min, 40min, 60min, and 120min and placed in 13mL test tubes. To these tubes, 1mL of DNS solution was promptly added to cease enzymatic activity. Once all samples were collected and dosed with DNS reagent, they were heated in a boiling water bath for 15min and then quickly cooled back down to room temperature with an ice water bath. The samples were then diluted with 8mL of DI water for a total volume of 10mL. A similar procedure was done to make a standard curve using known concentrations of glucose from 0 up to 300mg/dL. DNS method utilized as well as preparation of DNS reagent done as described in Miller (1959) with slight modifications. Samples and standards were read on a spectrophotometer (Evolution 300, Thermo Scientific Inc., Barrington, IL) at 576nm to determine glucose concentration. Before testing the samples, internal standards consisting of digestive enzymes with no bread, were used to screen out any effect of the enzymes on DNS readings. Total glucose available at end of digesting run was calculated by multiplying final concentration with final volume and subtracting calculated glucose levels from past samplings as shown in the following equation:

$$G = C_{120} \cdot 0.48 + 0.015(C_{120} + C_{60} + C_{40} + C_{20} + C_{10} + C_6 + C_3 + C_0)$$
where C is concentration in mg/dL and the subscripts are times in min samples were taken; 0.48 is the final volume in dL and 0.015 is the amount of sample taken in dL.

4. Intestinal phase: DIM

As with prior to the shaking water bath trial, sample was taken after gastric phase before intestinal enzymes were added to use for time zero. The intestinal enzymes were placed in a separate beaker and both it and the beaker with the digesta were taking to the DIM. Digesta and intestinal juice were pumped into the model at a constant

combined rate of 10mL/min. This was done at 5 mL/min for both entering gastric digesta and intestinal/bile juice due to the 1:1 ratio of salivary/gastric juice volume to duodenal/bile juice. For a larger test meal, it's recommended that the digesta flow rate be increased and duodenal/bile flow rate decreased to account for greater volume of food/salivary juice/gastric juice compared to volume of duodenal/bile juice. As with previous trials, the DIM is prefilled with liquid. In the case of these trials, a 7.4 pH sodium phosphate buffer was used to fill the membrane and prime the tubes. This buffer was also used as the recipient fluid. The overall volume of gastric digesta and duodenal/bile to perfuse into the model came to 62 mL. With the test flow rate of 10mL/min, complete perfusion of digesta and enzymes into the model was about six minutes. During the first 6 minutes, the sodium phosphate buffer used to fill the membrane was displaced back into its beaker. Around the 6 min mark, the buffer in the beaker was slowly added to both the digesta beaker and the duodenal/bile beaker. The fill/return tube was then secured on the rim of the digesta beaker. After about 3 min, the collection tube for the duodenal/bile juice was moved to the digesta beaker and little remaining buffer solution collected in duodenal/bile beaker was added to digesta beaker. From this point till the end of the trial, the model was recirculating. Samples were taken via the sampling tube inserted into the membrane at the top of the model. The tube holds approximately 8mL so when taking samples, first 8-10 mL were collected and returned to digesta beaker for reuptake and then 1.5 mL samples were taken. This only needed to be done for all the samples after the 3 min sample was taken. This was done to clear the tube of stagnant fluid. Samples were also collected from the recipient fluid at the same time periods in order to calculate absorption of glucose during digestion.

The DNS method was utilized to stop the enzyme and to measure glucose concentration. Due to the differences in overall volume between the two methods, 60 mL for shaking water bath and 500 mL for DIM, it was decided to use total glucose as illustrated above with the shaking water bath. The total glucose had to also be determined on the recipient side of the DIM so that total glucose available could be determined. The total glucose available was then compared between all four experimental conditions as well as digestion method. Due to the greater volume used in the DIM, the concentration of enzyme was reduced but so too was the food matrix concentration.



Figure 4.3: Model during digestion trial.

Results and Discussion

The results of total available glucose were summarized in figure 4.4 below. It shows a change both in digestion efficiency between shaking water bath and DIM digestion as well as marked reduction in glucose availability with bile salts included. Not much difference was noted when including the gastric enzymes. That was not unexpected giving the acidic conditions of stomach digestion and the enzymes produced

therein were meant more for protein breakdown. It's possible that with more complex food matrices with higher protein content could influence starch digestion if gastric enzymes don't get utilized to break down proteinaceous food prior to simulated intestinal digestion. It was shown that the addition of bile salts to simulated digestion as expected lowered glucose availability. The exact mechanism for this inhibition has been theorized to do with the helical arrangement of amylopectin binding bile and preventing amylase from binding (Takahama and Hirota 2011). It should be noted though that even with the ratio of enzymes to food being the same between both trials, the greater volume of the DIM would be expected to positively affect digestion efficiency. The greater volume coupled with the constant absorption of glucose in the recipient serum in the DIM for the first hour (figure 4.5) ensures that the amylase enzymes in pancreatin were not as quickly regulated by glucose product as with the shaking water bath. The general leveling off of glucose observed in the digesta in the shaking water bath trials could be explained positive feedback regulation of amylase by the product glucose, which in the smaller volume used in the shaking water bath and with no active removal of glucose by absorption, would cause a higher glucose concentration to enzyme ratio that would greatly reduce or halt starch digestion. It should be noted here that slight water uptake was observed with these trials and had to be accounted for in calculating total glucose. This shows the potential for the DIM to actively remove water from digesta like what is done in actual small intestine.

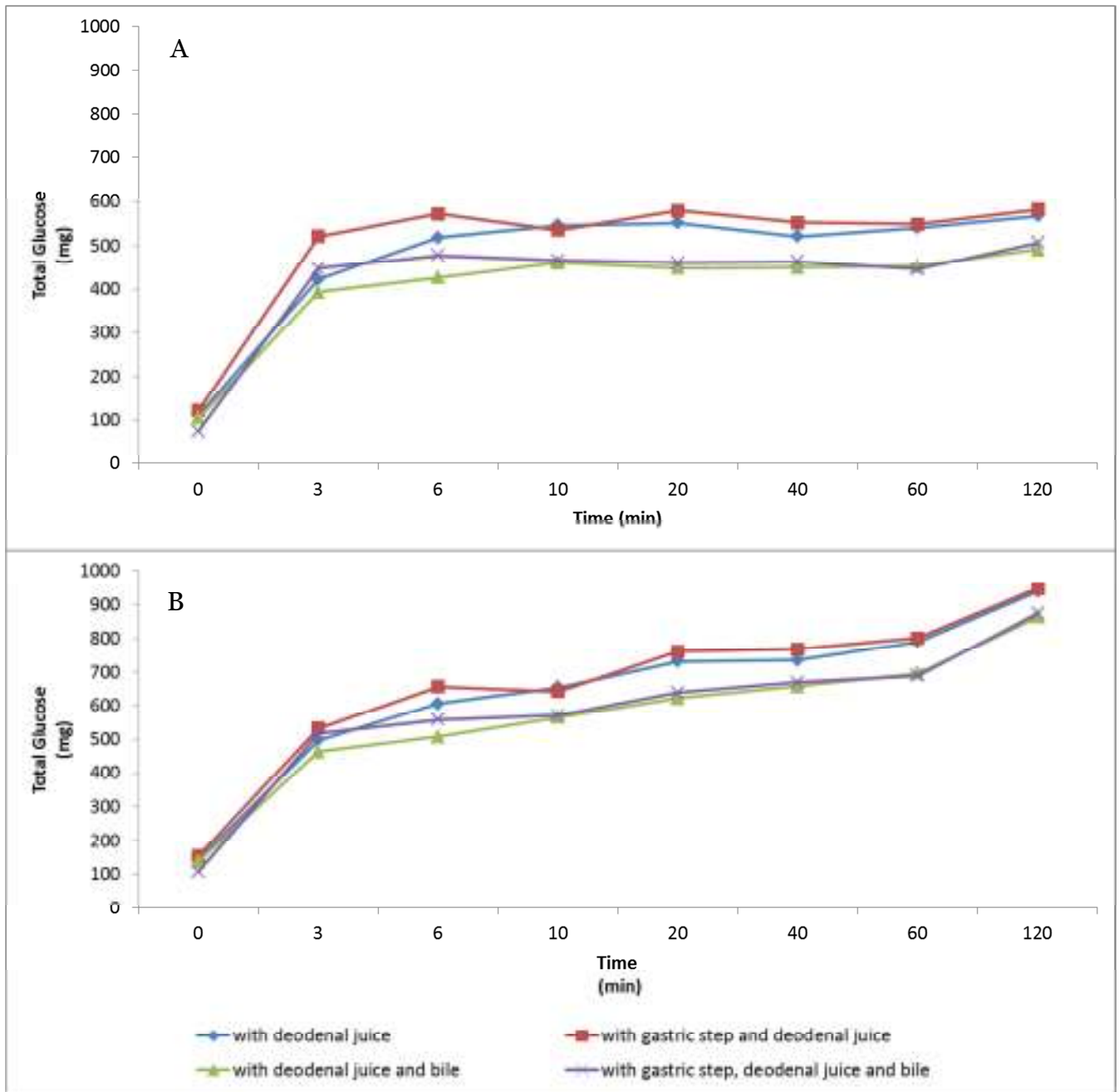


Figure 4.4: Results of total glucose at each time point in digesta. A. Shaking water bath. B. DIM results. For total glucose in DIM, glucose totals in recipient fluid were added back.

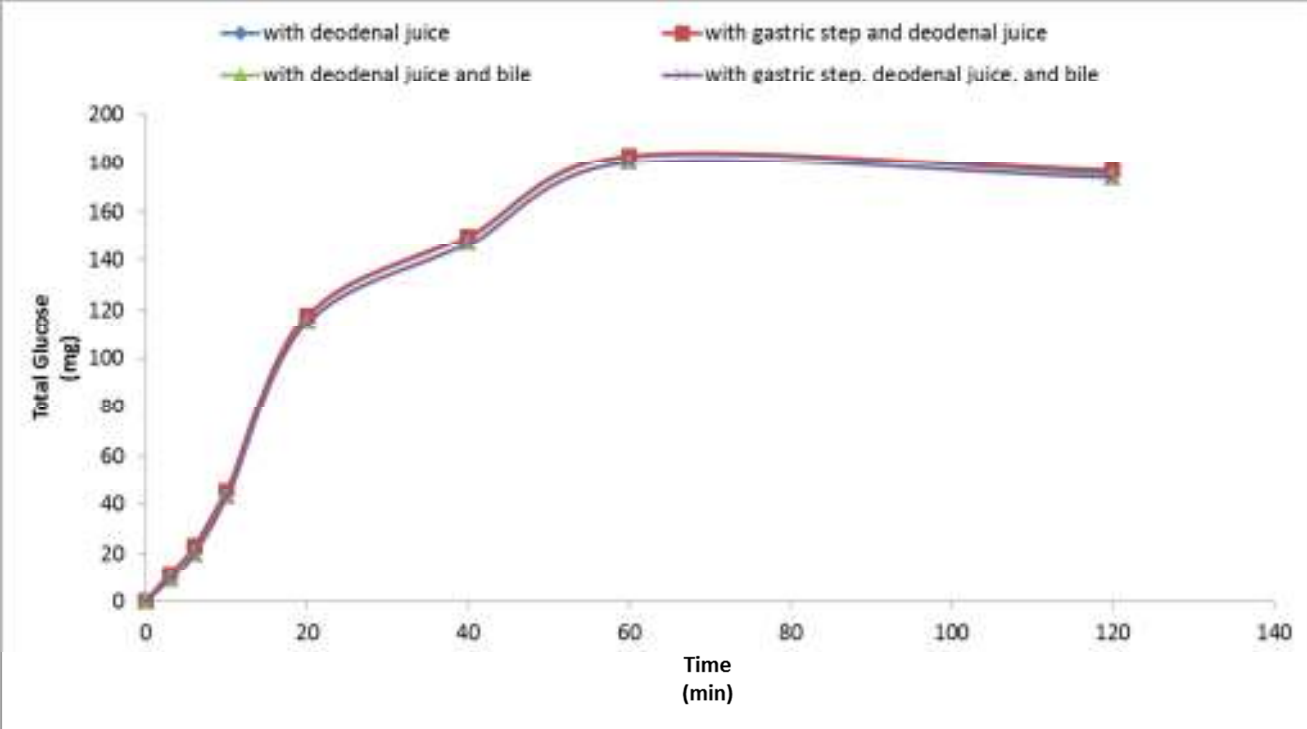


Figure 4.5: Absorbed glucose in DIM recipient serum.

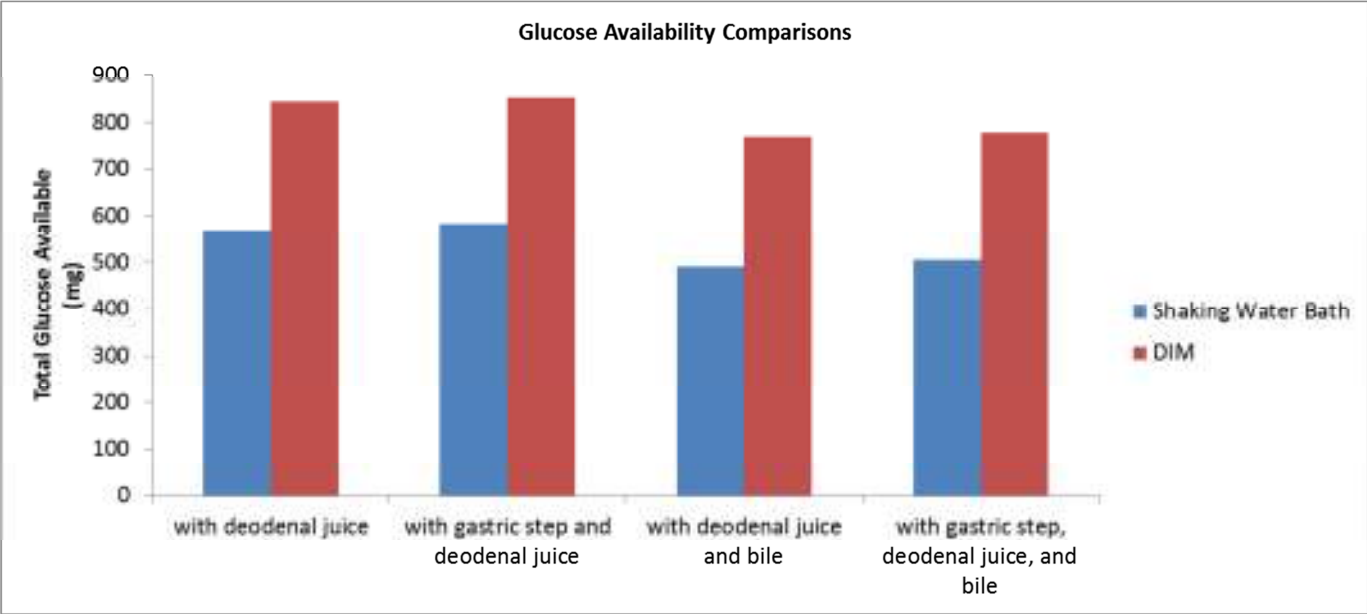


Figure 4.6: Total glucose results after 2h of digestion trials summarized.

Conclusions

It can be seen clearly from the results that the DIM model is more efficient when it comes to starch digestion. In all four conditions, there was significantly more glucose made available for absorption with the DIM. During water bath and DIM digestion, the introduction of bile salts reduced the amount of glucose availability. This has implications for blood sugar control and obesity if similar compounds such as polyphenols can be utilized to inhibit the breakdown of starch in the diet. Also shown in these trials was the importance of having an active mechanism for glucose absorption for simulating long-term intestinal digestion as glucose build up will itself begin to inhibit starch digestion when its concentration exceeds that of enzyme concentration, as shown in the result of shaking water bath. It also should be noted that multiple passes were made through the DIM. Given that the length of the DIM membrane is about twice that of the human duodenum, multiple passes may be utilized to not only simulate all the duodenum and part of the jejunum but also the entire length of the small intestine with good accuracy. Also with evidence of active water reuptake, it may be possible to better simulate the water reuptake function of the small intestine by increasing osmotic pressure across the membrane by salting the recipient fluid.

References:

- Barrett KE, Brooks HL, Boitano S, Barman SM. 2010. Section V Gastrointestinal Physiology. Ganong's Review of Medical Physiology 23rd Edition ed: McGraw Hill Medical. p. 429-87.
- Hur S, Decker E, McClements D. 2009. Influence of initial emulsifier type on microstructural changes occurring in emulsified lipids during *in vitro* digestion. Food Chemistry 114(1):253-62.
- Kim Y, Jeong Y, Wang M, Lee W, Rhee H. 2005. Inhibitory effect of pine extract on alpha-glucosidase activity and postprandial hyperglycemia. Nutrition 21(6): 756-61.
- Miller GL. 1959. Use of dinitrosalicylic acid reagent for determination of reducing sugar. Analytical Chemistry 31(3):426-8.
- Takahama U, Hirota S. 2010. Fatty Acids, Epicatechin-Dimethylgallate, and Rutin Interact with Buckwheat Starch Inhibiting Its Digestion by Amylase: Implications for the Decrease in Glycemic Index by Buckwheat Flour. Journal of Agricultural and Food Chemistry 58(23):12431-9.
- Takahama U, Hirota S. 2011. Inhibition of Buckwheat Starch Digestion by the Formation of Starch/Bile Salt Complexes: Possibility of Its Occurrence in the Intestine. Journal of Agricultural and Food Chemistry 59(11):6277-83.
- Versantvoort C, Kamp Evd, Rempelberg C. 2004. Development and applicability of an *in vitro* digestion model in assessing the bioaccessibility of contaminants from food. RIVM.
- Zahnley J. 1984. Stability of enzyme-inhibitors and lectins in foods and the influence of specific binding interactions. Advances in Experimental Medicine and Biology 177:333-65.

Chapter 5: Overall Conclusions

The DIM was developed as a more robust *in vitro* digestion tool as a means to accurately run digestion trials without having to resort to *in vivo* trials. The DIM incorporates realistic simulation of sedimentation and orientation to improve accuracy of digestion simulations. The pressure profiles generated within the DIM shows great similarities with the pressure profiles obtained with *in vivo* trials. By performing an absorption trial with glucose solution, perceived permeability values for the membrane used in the DIM were calculated. These values were then compared to perfusion studies done *in vivo* and values found for permeability were in good agreement, especially when comparing the mannitol *in vivo* data with the glucose DIM data.

By utilizing methylene blue solution, perceived permeability for the membrane used in the DIM was calculated. The kinetics information about propagation and absorption was obtained with the help of the DIM, which is useful for understanding the food digestion process. The results of these trials were backed up by *in vivo* data and thus by utilizing the proper parameters, the DIM can accurately simulate digestion in the human small intestine.

It can be seen from the results of bread digestion trials using the DIM model is more efficient when it comes to starch digestion than using a shaking water bath. More glucose was made available for absorption with the DIM. This study also shows that an active mechanism for glucose absorption is important for simulating long-term intestinal digestion as glucose build up will itself begin to inhibit starch digestion when its concentration exceeds that of enzyme concentration. Given that the length of the

DIM membrane is about twice that of the human duodenum, multiple passes may be utilized to not only simulate all the duodenum and part of the jejunum but also the entire length of the small intestine with good accuracy. Some proposed improvements to the DIM that would be beneficial include mounting the main body of the model on a movable stand to not only make the protocol for model set up easier but also possibly simulate more different orientations, perhaps even installing a stepper motor controlled by programmable logic to tilt the main body of the model at different times during a digestion run.